CHAPTER 5

Band Structure and Quantum Transport Phenomena in Narrow-Gap Diluted Magnetic Semiconductors

J. Kossut

INSTITUTE OF PHYSICS, POLISH ACADEMY OF SCIENCES
WARSAW, POLAND

I. Introduction

In this chapter, we deal with narrow-gap diluted magnetic semiconductors (DMS), known also as semimagnetic semiconductors. We focus our attention on their band structure in the presence of a strong, quantizing magnetic field. The small values of the effective masses, characteristic of narrow-gap semiconductors, make them particularly suitable for investigations in the

ISBN 0-12-752125-9

quantum regime. In fact, the diluted magnetic semiconductors with a narrow forbidden gap were probably the first to be studied experimentally (Delves, 1963 and 1966; Morrissy, 1973). Their puzzling properties remained largely unexplained until the model of their band structure has been proposed (Jaczynski *et al.*, 1978; Bastard *et al.*, 1978; see also the review paper by Galazka and Kossut, 1980). The model, based on the $\mathbf{k} \cdot \mathbf{p}$ approximation, assumes that two electronic subsystems can be distinguished. The first contains mobile delocalized electrons from the conduction and/or uppermost valence band. These electrons, which can be described in terms of the virtual crystal approximation, are mostly responsible for electrical and optical properties. The second subsystem consists of electrons from the 3d shells of, typically, Mn ions. It is assumed that these produce localized magnetic moments. The degree of the localization of the magnetic ions is still disputed. Only recently the calculation based on the coherent potential approximation started to give insight into this problem (Hass and Ehrenreich, 1983). The latter electronic subsystem is responsible for the magnetic properties of DMS. The interaction between these two subsystems produces a spectrum of anomalies in the electrical and optical properties of diluted magnetic semiconductor. The reciprocal influence of mobile electrons is more difficult to detect, because it would require much greater electron concentrations than usually met in semiconductors. Such an influence has been recently detected in a quaternary mixed crystal $Pb_{1-x-y}Sn_xMn_yTe$ (Story *et al.*, 1985). We shall assume throughout this chapter that no spontaneous magnetization exists in the materials considered, i.e., the ordering of the localized moments is always induced by an external magnetic field.

The plan of this chapter is the following: Part II discusses in detail the interaction between two electronic subsystems. Next, Part III presents models of the band structure in a magnetic field for narrow gap DMS with the zinc blende lattice structure (e.g., $Hg_{1-x}Mn_xTe$). Part IV deals with experimental results for various DMS (including those with NaCl and tetragonal crystal structures) obtained in the course of investigations of quantum transport phenomena, mostly the Shubnikov de Haas effect. In this chapter we shall put stress on those features that are unique for the diluted magnetic semiconductors and that support the proposed model of the band structure. The final Part V is devoted to a discussion of a preliminary investigation of quasi two-dimensional electronic systems in diluted magnetic semiconductors.

We do not attempt to quote here the values of all important band structure parameters determined for the narrow-gap diluted magnetic semiconductors. We refer the readers to the tables of these quantities compiled by Galazka and Kossut (1983).

II. Exchange Interaction Between Mobile s or p Carriers and Localized 3d or 4f Electrons in Semiconductors

1. Interaction Hamiltonian

The exchange interaction between mobile, s-like band electrons and localized electrons from partially filled 3d (or 4f) shells was first considered in transition (or rare-earth) metals. Early ideas of Zener (1951a–c) and Vonsovskii and Turov (1953) led to the development of the so-called s–d (or s–f) model. The case of rare-earth metals was particularly stimulating in this development, since magnetic properties of these materials could hardly be explained in terms of direct exchange interaction involving the overlap of 4f wave functions localized on neighboring rare-earth atoms. The localization of these wave functions is so strong (thus their overlap so small) that the estimated values of the direct exchange constants are far too small to account, e.g., for magnetic transition temperatures observed. Therefore indirect coupling between the localized magnetic moments of rare-earth ions via conduction electrons was invoked in order to explain the observed magnetic behavior. Several authors dealt with the problem of the form of this coupling (see, e.g., Vonsovskii and Turov, 1953; Kasuya, 1955; Abrahams, 1955; Yosida, 1957; Mitchell, 1957). It was found that the exchange interaction between the conduction electrons and 3d or 4f electrons (i.e., those responsible for the formation of localized magnetic moments) can be represented by a simple Heisenberg-like formula

$$H_{sd} = \sum_n J(\mathbf{r} - \mathbf{R}_n)\mathbf{s} \cdot \mathbf{S}_n \tag{1}$$

where $\mathbf{s}$ is the spin operator of an s-electron at position $\mathbf{r}$, $\mathbf{S}_n$ is the total spin operator of a 3d (or 4f) shell at $\mathbf{R}_n$ and $J(\mathbf{r} - \mathbf{R}_n)$ is an appropriate exchange constant (a constant term has been omitted in Eq. (1)). It was argued that the function $J(\mathbf{r} - \mathbf{R}_n)$ is strongly peaked around $\mathbf{R}_n$ and quickly vanishes away from this point, reflecting the localized nature of the 3d (or 4f) electrons. The form given by Eq. (1) is not the most general one, since several assumptions have been made during its derivation. First, a constant number of electrons in the 3d (4f) shell associated with a given ion was assumed. In other words the magnitude of the localized spin was taken to be constant. It is possible to generalize the Hamiltonian and avoid this limitation (e.g., Vonsovskii and Svirskii, 1964; Irkhin, 1966).

However we shall restrict our attention to the simpler case, assuming a constant value of the localized spin, as experimental data obtained on diluted magnetic semiconductors seem to suggest.

The second assumption made when deriving Eq. (1) concerns the validity of the description of the localized moments in terms of the spin eigenvalues. Such description often requires the use of a total angular momentum $\mathbf{J}_n$ instead of the spin only. It was shown by Liu (1961) that even in such a case a simple form involving the scalar product can be retained if $\mathbf{S}_n$ in Eq. (1) is replaced by $\mathbf{J}_n$ and the coupling coefficient $J(\mathbf{r} - \mathbf{R}_n)$ is slightly redefined:

$$H_{\mathrm{sd}} = \sum_n J(\mathbf{r} - \mathbf{R}_n)\mathbf{s} \cdot \mathbf{J}_n . \tag{2}$$

Conversely, when mobile band electrons are subject to a strong spin-orbit interaction (as is commonly the case in semiconductors, e.g., in the valence band p-like states in zinc blende III-V and II-VI compounds), it is more proper to label their states using eigenvalues of total angular momentum $\mathbf{j}$. Then, the coupling Hamiltonian (that in this case corresponds to p-d coupling) can be conveniently expressed as:

$$H_{\mathrm{pd}} = \sum_n J(\mathbf{r} - \mathbf{R}_n)\mathbf{j} \cdot \mathbf{S}_n . \tag{3}$$

All expressions quoted so far are isotropic. It can be shown that this is only an approximation, valid if spatial extensions of 3d (4f) wave functions are small compared to the de Brolie wavelength of mobile s- or p-electrons. Only then the mobile carriers do not "feel" an anisotropic character of 3d (4f) functions. This condition is sometimes not easy to meet in metals. Therefore, a generalization of Eq. (1) was found by Kaplan and Lyons (1963) that is explicitly anisotropic. In semiconductors, however, the mobile carriers which usually play a role, are characterized by much smaller values of momenta $\mathbf{k}$ than in metals; that is, they have longer de Brolie wavelengths. This fact justifies the use of the isotropic expression (1) in our further considerations of diluted magnetic semiconductors.

2. Exchange Constants

We shall now turn our attention to the nonlocal "potential" $J(\mathbf{r} - \mathbf{R}_n)$ appearing in Eq. (1). All papers quoted in the preceding section defined rather the Fourier transform of $J(\mathbf{r} - \mathbf{R}_n)$ than this function itself. This transform can be written as

$$J(\mathbf{k}, \mathbf{k}') = -2 \int \psi^*_{nk}(\mathbf{r})\phi^*_{\mathrm{d}}(\mathbf{r}')V(\mathbf{r} - \mathbf{r}')\psi_{n'k'}(\mathbf{r}')\phi_{\mathrm{d}}(\mathbf{r})d^3r'd^3r \tag{4}$$

where ψ_{nk} denotes the spin-independent part of the wave function of a mobile band electron in the n-th band with a wave vector $\mathbf{k}$, ϕ_d is an appropriate wave function of 3d (or 4f) electrons (possibly integrated over all spatial variables but one) and $V(\mathbf{r} - \mathbf{r}')$ is the electrostatic interaction between the electrons. One may interpret Eq. (4) as a direct exchange interaction between the particles in question. A problem arises concerning the actual dependence of $J(\mathbf{k}, \mathbf{k}')$ on the mobile electron momenta $\mathbf{k}$ and $\mathbf{k}'$. This dependence is difficult to extract from Eq. (4) in a general case. In metals, one often argues that, since only the electrons from the Fermi surface are important in the majority of physical situations, it is possible to replace $\mathbf{k}$ and $\mathbf{k}'$ in Eq. (4) by their values at this surface; that is, for a spherical Fermi surface they can be replaced by a single parameter k_F. Thus, one is left with only one exchange constant. Its value has been estimated theoretically on the basis of Eq. (4) by several authors (e.g., Izyumov and Noskova, 1962; Kasuya, 1966; Kasuya and Lyons, 1966; Watson and Freeman, 1966 and 1969). These estimations give values in the range 10^{-3}–10^{-1} eV.

Slightly different reasoning has to be invoked in the case of semiconductors, which is of interest to us here. A most widely used description of band electrons in semiconductors is in terms of the $\mathbf{k} \cdot \mathbf{p}$ perturbation approach (Luttinger and Kohn, 1955). Usually, one is interested only in electrons that are in the vicinity of band extrema. Therefore, the wave function ψ_{nk} is sought as a combination of the wave functions at various band edges u_n (n is the band index; for the sake of simplicity let us assume now that the band extrema occur at $k = 0$),

$$\psi_{nk} = \sum_n a_n(\mathbf{k}) u_n(\mathbf{r}) e^{i\mathbf{k}\cdot\mathbf{r}}, \tag{5}$$

where $a_n(\mathbf{k})$ are coefficients of the combination. The sum in Eq. (5) can often be restricted to only a few terms. This is particularly true in the case of narrow-gap semiconductors. Then the coefficients $a_n(\mathbf{k})$ can be found exactly together with their explicit dependence on the wave vector $\mathbf{k}$. Inserting wave functions (5) into (4), we obtain

$$J(\mathbf{k}, \mathbf{k}') = -2 \sum_{nn'} a_n^*(\mathbf{k}) a_{n'}(\mathbf{k}') \times \int e^{-i\mathbf{k}\cdot\mathbf{r}} u_n^*(\mathbf{r}) \psi_d^*(\mathbf{r}') V(\mathbf{r} - \mathbf{r}') e^{i\mathbf{k}'\cdot\mathbf{r}'} u_{n'}(\mathbf{r}') \psi_d(\mathbf{r}) d^3r d^3r'. \tag{6}$$

As we can see a part of the $\mathbf{k}, \mathbf{k}'$ dependence is already taken out from the integral. The remaining k-dependence is of lesser importance. As we

mentioned above, the wave vectors of band electrons usually encountered in semiconductors are rather small in magnitude. Because of the strongly localized character of the ϕ_d functions, the main contribution to the integral in Eq. (6) comes from the region of small r and r'. In this region the exponential factors in the integrand can be approximated by 1. So, the whole dependence of $J(\mathbf{k}, \mathbf{k}')$ on $\mathbf{k}, \mathbf{k}'$ is now given by the factors $a_n^*(\mathbf{k})$ and $a_{n'}(\mathbf{k}')$. One may now define a set of basic exchange constants, all of them independent of $\mathbf{k}, \mathbf{k}'$ (Kossut, 1976)

$$J_{nn'} = -2 \int u_n^*(\mathbf{r}) \phi_d^*(\mathbf{r}') V(\mathbf{r} - \mathbf{r}') u_{n'}(\mathbf{r}') \phi_d(\mathbf{r}) d^3r d^3r'. \tag{7}$$

Moreover, when symmetry arguments are invoked, only the "diagonal" elements J_{nn} can be shown to be nonvanishing. We shall denote them by J_n. Two of these basic exchange constants are very commonly encountered in diluted magnetic semiconductors. They involve s-like electrons from what usually is a conduction band of Γ_6 symmetry in semiconductors with the zinc blende lattice, and p-like electrons from the Γ_8 symmetry band. Traditionally they are denoted, respectively, by α and β in the literature dealing with diluted magnetic semiconductors:

$$\alpha = J_{\Gamma_6} = \frac{1}{\Omega_0} \langle S|J|S \rangle \tag{8}$$

$$\beta = J_{\Gamma_8} = \frac{1}{\Omega_0} \langle X|J|S \rangle \tag{9}$$

where $u_{\Gamma_6} = \Omega_0^{-1/2} S(\mathbf{r})$ and $u_{\Gamma_8} = \Omega_0^{-1/2} X(\mathbf{r})$ while Ω_0 stands for the volume of a unit cell. The elements as $\langle S|J|S \rangle$, etc., commonly used in the literature, represent symbolically the integration indicated by Eq. (7) with appropriate wave functions u_n of the electron at the band edge.

In the course of various investigations of DMS it was established (see other chapters in this volume) that the constants α and β differed in sign: β turns out to be positive ("antiferromagnetic") while α is negative ("ferromagnetic"). Usually the absolute value of β is greater than α. On the basis of Eq. (7), on the other hand, one could expect a single sign ("ferromagnetic") for both constants.

Recently, two attempts to solve this puzzling fact have been published (Semenov and Shanina, 1981 and Bhattacharjee *et al.*, 1983). The first of these two papers notes that, apart from the term given by Eq. (4), there is also a contribution arising from the overlap integral of the 3d wavefunction and wavefunctions of the band electron (this contribution also leads to a

general form of the interaction Hamiltonian (3)). This contribution is opposite in sign to that given by the direct exchange mechanism represented by Eq. (4). This is of particular importance for p-like electrons, which usually form the valence band in semiconductors, while for s-like conduction band electrons it can be practically neglected. Therefore, it can explain the difference in sign of α and β. The importance of the overlap term in the case of p-like electrons follows from the fact that these electrons originate mainly from the anions (e.g., Te ions in $Cd_{1-x}Mn_xTe$). Therefore, the corresponding wave functions are peaked at the anion lattice sites (say, in a tight binding scheme), which are the nearest neighbors of a given Mn ion. Thus, the overlap of these functions and 3d wave functions of Mn may be appreciable.

On the other hand, the s-like electrons originate mainly from cation sublattice atoms, i.e., either from Mn atoms themselves or from more distant Cd or Mn ions. In the former case their wave functions are orthogonal to the 3d functions (same ion). In the latter situation the overlap produced must be smaller because of a greater distance between the ions. It is then concluded that in the case of the constant α the direct (ferromagnetic) exchange mechanism dominates, while the overlap contribution determines the value of β. Indeed, estimates by Semenov and Shanina (1981) give an order of magnitude for $|\alpha| \cong \beta = 0.1 \div 1$ eV and $\alpha < 0$. Note that our definition (1) differs in sign from the definition used by Semenov and Shanina.

A different approach to the problem of sign of α and β is taken in the paper by Bhattacharjee *et al.* (1983). It stresses the importance of hybridization of the localized d and the valence-band p electrons. On the basis of the virtual bound state approach (Anderson, 1961; Friedel, 1958), it is shown that the Anderson Hamiltonian (which by the Schrieffer and Wolff (1966) transformation is equivalent to the s-d model) for reasonable model parameters leads to a positive ("antiferromagnetic") exchange constant β for the p-like valence electrons. The hybridization is not effective in the case of α. This is partly because the virtual bound state due to d electrons falls into the valence band and is energetically quite distant from the conduction band. The energy denominators appearing in the theory reduce then quite strongly the contribution to α due to the hybridization. Also, the relevant hybridization matrix elements are smaller for s-like than for p-like electrons. Thus the normal direct exchange mechanism is mainly responsible for the value and sign of α, while an interplay between direct exchange and hybridization determines β.

It is difficult to decide at the present stage, which of the two approaches describes better the physical reality. None of the experiments (e.g., experiments on samples under hydrostatic pressure, which would affect the overlap integrals discussed by Semenov and Shanina, 1981) could distinguish

between the models. One is, then, still in a situation in which the relevant exchange constants have to be treated as phenomenological quantities, with values treated as adjustable parameters of the given model of a diluted magnetic semiconductor.

III. Band Structure of Narrow-Gap Diluted Magnetic Semiconductors in Quantizing Magnetic Fields

The majority of papers dealing with narrow-gap diluted magnetic semiconductors is devoted to alloys based on II–VI mercury compounds, e.g., $Hg_{1-x}Mn_xTe$ or $Hg_{1-x}Mn_xSe$. They were also the first studied experimentally in an extensive manner. Therefore, we describe here the band structure of these materials. We shall discuss briefly the band structure of tetragonal $(Cd_{1-x}Mn_x)_3As_2$ and DMS based on lead chalcogenides (or rather only the modifications of the general model associated with their different crystallographic symmetries), when we describe in the following sections the experimental results obtained for these materials.

Early investigations (Morrissy, 1973; Delves, 1963 and 1966) indicated that semiconducting properties of $Hg_{1-x}Mn_xTe$ cannot be entirely understood in terms of existing theoretical models that could be successfully applied to such semiconducting mixed crystals as $Hg_{1-x}Cd_xTe$. The unexplained features of $Hg_{1-x}Mn_xTe$ were a non-monotonic temperature behavior of the Shubnikov–de Haas oscillation amplitude (Morrissy, 1973) and the value of the spin-splitting of electrons and its temperature dependence observed in magneto-optical study of Bastard *et al.* (1978) (see also Rigaux, this volume). On the other hand, when no strong magnetic field was applied, the band structure of $Hg_{1-x}Mn_xTe$ appeared to be qualitatively the same as in $Hg_{1-x}Cd_xTe$, as indicated in the study of Stankiewicz *et al.* (1975). As in other narrow-gap materials with the zinc blende lattice symmetry, the minimum of the conduction band and the maximum of the valence band occur at the central point Γ of the Brillouin zone. There are three bands with similar energies (see Fig. 1): a fourfold degenerate band of Γ_8 symmetry, and doubly degenerate Γ_6 and Γ_7 symmetry bands. The sequence of these bands varies with the crystal composition. For low values of Mn mole fraction x, we deal with the so-called inverted band ordering (or symmetry-induced zero-gap configuration) depicted in Fig. 1a. For increasing values of x, Γ_6 valence band shifts upwards, and at $x = 0.065$ (at 4.2 K), it coincides with the position of the Γ_8 band (Fig. 1b). Above this semimetal–semiconductor transition point, Γ_6 band starts to form the conduction band (Fig. 1c) while the Γ_8 band becomes the light and heavy hole band. The energy gap E_g defined as the energy difference between Γ_8 and Γ_6 levels is then positive, and we are dealing with

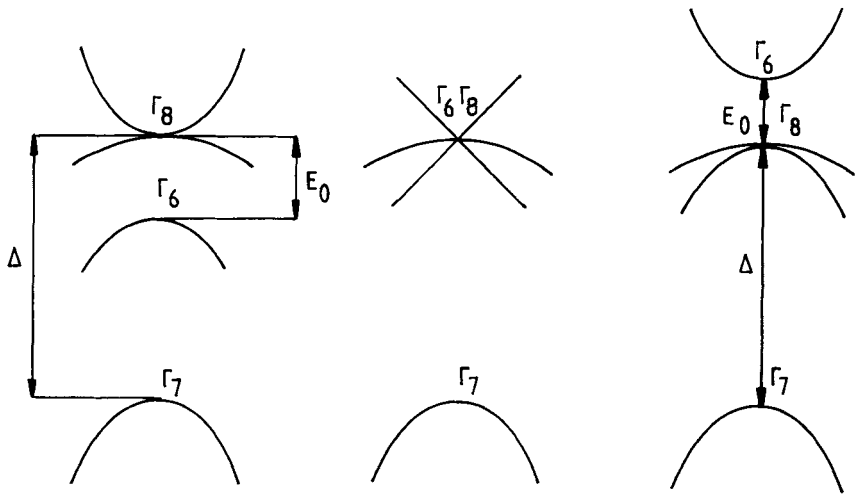

FIG. 1. The energy level scheme in the vicinity of the conduction and valence band edges in narrow-gap semiconducting mixed crystals with zinc blende structure: (a) inverted (zero-gap) band structure; (b) semimetal-semiconductor transition point; (c) open-gap structure.

the standard semiconducting band ordering. The variation of the energy gap with the crystal composition in $Hg_{1-x}Mn_xTe$ is shown in Fig. 2. The Γ_7 symmetry band (or spin–orbit split-off band) remains a deeper valence band.

It is well known from the work of Kane (1957) that the proper description of a narrow-gap semiconductor requires that at least the three bands Γ_6, Γ_7 and Γ_8, because of their energetic proximity, are considered at the same level of accuracy in a $\mathbf{k} \cdot \mathbf{p}$ treatment of the band structure. The remaining more remote bands, often referred to as "higher bands", may be treated in an approximative way. Their influence on the shape of the conduction and valence bands is usually evaluated with accuracy to terms proportional to k^2, where k is the electronic wave vector. Only in the case of HgSe, and of mixed crystals similar in composition to HgSe, does one have to include in the set of closely spaced (quasi-degenerate) bands also the nearest higher band of Γ_{15} (no spin notation) symmetry, as found by Mycielski *et al.* (1982). This fact is connected with the relation $E_g \approx 2/3\Delta$, where Δ is the spin–orbit splitting (or the distance between Γ_8 and Γ_7 bands), that is fulfilled in HgSe. However, a very steep slope of the E_g vs. x relationship in $Hg_{1-x}Mn_xSe$ (Dobrowolska *et al.*, 1981) limits this "anomalous" region to $x \leq 0.0005$. Also, the modifications due to such enlargement of the quasi-degenerate set of bands concern mainly the Γ_6 band (light holes) and therefore are possibly important in an analysis of the interband magnetoabsorption

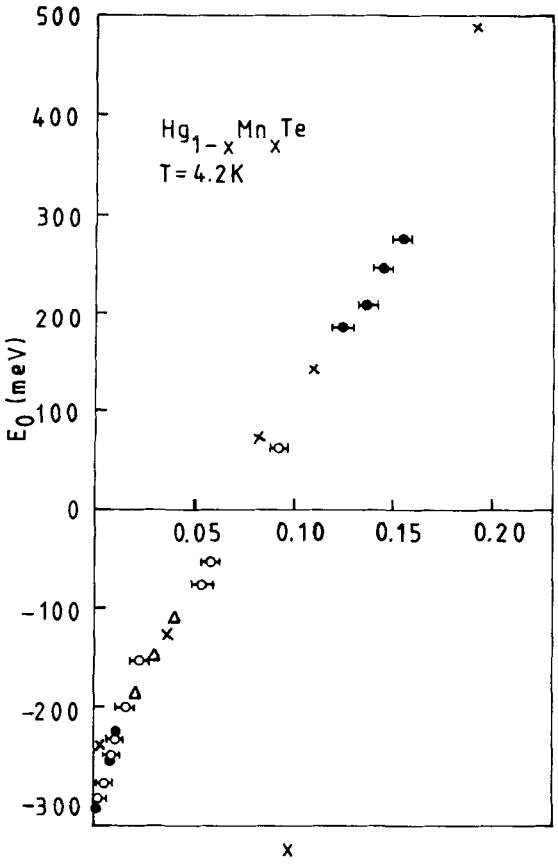

FIG. 2. Variation of the energy gap with composition of $Hg_{1-x}Mn_xTe$. [After Galazka and Kossut (1983).]

experiments. In this chapter, which is focused mainly on the magneto-transport phenomena in n-type DMS, we shall neglect this complication in further considerations.

There exist in the literature on narrow-gap semiconductors the simplified models of their band structure in a presence of a strong magnetic field. In particular, the so-called quasi-Ge model of Luttinger (1956) includes into the quasi-degenerate set of states only the Γ_8 band. The three-band model (e.g., Kacman and Zawadzki, 1971) although considering in detail all closely positioned Γ_6, Γ_7 and Γ_8 bands, neglects totally the influence of the higher bands. The advantage of these models lies in the fact that they can be solved analytically. However, their applicability is only of limited range.

In particular, the spin-splitting of electronic states, a quantity of primary importance in the case of diluted magnetic semiconductors, is only approximately rendered by these models. Moreover, when the exchange interaction between electrons from the Γ_6, Γ_7, Γ_8 bands and 3d electrons forming magnetic moments localized on Mn ions is taken into account, even these simpler models cannot, in general, be solved in an analytic way without further simplifications. Therefore, we shall base our further calculations on the model of Pidgeon and Brown (1966) that, although only numerically soluble for standard narrow-gap semiconductors, takes fully into account all the important bands.

The Pidgeon–Brown model treats within the $\mathbf{k} \cdot \mathbf{p}$ approximation the bands Γ_6, Γ_7, Γ_8 as quasi-degenerate and accounts for the higher bands in a perturbative way by means of several parameters. As is usually the case when starting a $\mathbf{k} \cdot \mathbf{p}$ calculation, one has to define the set of basis functions at the band extrema (often called the Luttinger–Kohn amplitudes). We choose this set in a standard form for the crystals of zinc blende symmetry.

$$
\begin{aligned}
\Gamma_6 &\begin{cases} u_1 = S\uparrow, \\ u_2 = iS\downarrow, \end{cases} \\
\Gamma_8 &\begin{cases} u_3 = \frac{1}{\sqrt{2}}(X + iY)\uparrow, \\ u_4 = i\frac{1}{\sqrt{2}}(X - iY)\downarrow, \\ u_5 = \frac{1}{\sqrt{6}}[(X - iY)\uparrow + 2Z\downarrow], \\ u_6 = i\frac{1}{\sqrt{6}}[(X + iY)\downarrow - 2Z\uparrow], \end{cases} \\
\Gamma_7 &\begin{cases} u_7 = i\frac{1}{\sqrt{3}}[-(X - iY)\uparrow + Z\downarrow], \\ u_8 = \frac{1}{\sqrt{3}}[(X + iY)\downarrow + Z\uparrow], \end{cases}
\end{aligned}
\tag{10}
$$

where the Luttinger–Kohn amplitude S transforms under the operations from the T_d group as an atomic s-like function and the amplitudes X, Y, and Z as atomic p_x, p_y, p_z-like functions, respectively. The symbols $\uparrow$ and $\downarrow$ denote the Pauli spinors. The matrix elements of the $\mathbf{k} \cdot \mathbf{p}$ Hamiltonian in the

presence of the external magnetic field form an 8×8 matrix. Rearranging the sequence of the basis functions to $u_1, u_3, u_5, u_7, u_2, u_4, u_6, u_8$ we can write this matrix (Leung and Liu, 1973) as

$$D = \begin{bmatrix} D_a & D_c \\ D_c^\dagger & D_b \end{bmatrix}, \tag{11}$$

where the matrices D_a, D_b, and D_c are defined by Eqs. (14), (15), and (16) with the following notation

$$C = \frac{\hbar^2}{m_0}, \tag{12}$$

$$s = \frac{eH}{\hbar c}, \tag{13}$$

with m_0 being the free electron mass.

$$D_a = \begin{bmatrix} E_g + 2CsF(N + \frac{1}{2}) & iP\sqrt{s}a^+ \\ + Cs(N + 1) + (F + \frac{1}{2})Ck_z^2 & \\ & -Cs[(\gamma_1 + \gamma_2)(N + \frac{1}{2}) \\ D_{a_{12}}^* & + \frac{3}{2}\kappa] + (\gamma_2 - \frac{1}{2}\gamma_1)Ck_z^2 \\ D_{a_{13}}^* & D_{a_{23}}^* \\ D_{a_{14}}^* & D_{a_{24}}^* \end{bmatrix}$$

$$\begin{bmatrix} iP\sqrt{\frac{s}{3}}a & P\sqrt{\frac{2}{3}s}a \\ -\frac{1}{2}Cs\sqrt{3}[(\gamma_2 - \gamma_3)a^{+2} & iCs\sqrt{\frac{2}{3}} \\ + (\gamma_2 + \gamma_3)a^2] & \times [(\gamma_2 - \gamma_3)a^{+2} + (\gamma_2 + \gamma_3)a^2] \\ - Cs[(\gamma_1 - \gamma_2)(N + \frac{1}{2}) & iCs\sqrt{2}[\gamma_2(N + \frac{1}{2}) - \frac{1}{2}\kappa - \frac{1}{6}] \\ - \frac{1}{2}\kappa] - (\gamma_2 + \frac{1}{2}\gamma_1)Ck_z^2 & - i\sqrt{2}\gamma_2 Ck_z^2 \\ & - Cs[\gamma_1(N + \frac{1}{2}) - \kappa - \frac{1}{2}] \\ D_{a_{34}}^* & - \frac{1}{2}\gamma_1 Ck_z^2 - \Delta \end{bmatrix} \tag{14}$$

$$D_b = \begin{bmatrix} E_g + 2CsF(N+\frac{1}{2}) + CsN + (F+\frac{1}{2})Ck_z^2 & i\sqrt{s}Pa & \\ D^*_{b_{12}} & -Cs[(\gamma_1+\gamma_2)(N+\frac{1}{2}) - \frac{3}{2}\kappa] + (\gamma_2 - \frac{1}{2}\gamma_1)Ck_z^2 & \\ D^*_{b_{13}} & D^*_{b_{23}} & \\ D^*_{b_{14}} & D^*_{b_{24}} & \end{bmatrix}$$

$$\begin{bmatrix} i\sqrt{\frac{s}{3}}Pa^+ & \sqrt{\frac{2}{3}}sPa^+ \\ -\frac{1}{2}Cs\sqrt{3}[(\gamma_2+\gamma_3)a^{+2} + (\gamma_2-\gamma_3)a^2] & iCs\sqrt{\frac{2}{3}}[(\gamma_2+\gamma_3)a^{+2} + (\gamma_2-\gamma_3)a^2] \\ -Cs[(\gamma_1-\gamma_2)(N+\frac{1}{2}) + \frac{1}{2}\kappa] - (\frac{1}{2}\gamma_1+\gamma_2)Ck_z^2 & iCs\sqrt{2}[\gamma_2(N+\frac{1}{2}) + \frac{1}{2}\kappa + \frac{1}{6}] - i\sqrt{2}\gamma_2 Ck_z^2 \\ D^*_{b_{34}} & -Cs[\gamma_1(N+\frac{1}{2}) + \kappa + \frac{1}{2}] - \frac{1}{2}\gamma_1 Ck_z^2 - \Delta \end{bmatrix} \tag{15}$$

$$D_c = \begin{bmatrix} 0 & 0 & \sqrt{\frac{2}{3}}Pk_z & i\frac{1}{\sqrt{3}}Pk_z \\ 0 & 0 & iC\sqrt{6s}\gamma_3 k_z a & -C\sqrt{3s}\gamma_3 k_z a^+ \\ \sqrt{\frac{2}{3}}Pk_z & -iC\sqrt{6s}\gamma_3 k_z a & 0 & -3C\sqrt{s}\gamma_3 k_z a^+ \\ -\frac{i}{\sqrt{3}}Pk_z & -C\sqrt{3s}\gamma_3 k_z a & -3C\sqrt{s}\gamma_3 k_z a^+ & 0 \end{bmatrix} \tag{16}$$

The operators a and a^+ in Eqs. (14)–(16) are the harmonic oscillator lowering and raising operators, respectively, defined as

$$a^+ = \frac{1}{\sqrt{2s}}(k_x + ik_y), \tag{17}$$

$$a = \frac{1}{\sqrt{2}s}(k_x - ik_y), \tag{18}$$

and

$$N = a^+ a. \tag{19}$$

P is the interband momentum matrix element

$$P = -\frac{i\hbar}{m_0}\langle S \,|\, p_x \,|\, X\rangle, \tag{20}$$

and the parameters γ_1, γ_2, γ_3, κ, and F describe the coupling to the higher bands. The eigenvectors of the matrix (11) can be sought in the form

$$F_n = (L_y L_z)^{-1/2} \exp[i(k_y y + k_z z)] \begin{bmatrix} a_1 \phi_{n-1} \\ a_3 \phi_{n-2} \\ a_5 \phi_n \\ a_7 \phi_n \\ a_2 \phi_n \\ a_4 \phi_{n+1} \\ a_6 \phi_{n-1} \\ a_8 \phi_{n-1} \end{bmatrix} \tag{21}$$

where $\phi_n(\xi)$ is the harmonic oscillator eigenfunction of the variable $\xi = x - k_y/s$.

Acting with the matrix (11) on the eigenvector given by Eq. (21) we obtain the matrix which can be diagonalized numerically in order to find the eigenvalues for a given magnetic field and harmonic oscillator quantum number n and k_z. Let us note further that if we put $k_z = 0$ (i.e., we are interested in the energy positions of the Landau subband minima), the whole matrix D can be partially decomposed into two noninteracting matrices D_a and D_b. The matrix D_c, Eq. (16), is then equal to zero. We are then left with two independent eigenproblems, each 4×4 dimensional, the solution of which gives us in general two sets (a- and b-set) of eigenenergies. Note that, in the case of the Landau quantum number $n = -1$ one has to put all coefficients a_i in Eq. (21) equal to zero except for a_4. The single energy level obtained in such case, which is very easy to find, corresponds to the uppermost heavy hole valence band Landau level. Similarly, when $n = 0$ one has to put $a_1 = a_3 = a_6 = a_8 = 0$ and for $n = 1$: $a_3 = 0$.

Having described in detail the model of the band structure of a narrow-gap semiconductor, let us return to the problem of a diluted magnetic semiconductor. As mentioned before one could not hope to describe the band structure in this case simply by an appropriate choice of a set of parameters

defined previously in this section. This fact is probably best illustrated by a simultaneous analysis of the effective mass and spin splitting of the conduction electron. The model described above predicts that the effective mass at the bottom of the conduction band is determined mainly by the ratio E_g/P^2, the dependence on other parameters being less significant. Similarly, the electronic g-factor, that describes the spin splitting, is roughly determined by m_0/m^* (where we assumed $\Delta = \infty$). Thus, for a given crystal composition, i.e., for a given E_g and P (P being only slightly sensitive to the actual value of Mn mole fraction x), both the effective mass and the g-factor should be interrelated. The measured values of the effective masses in $Hg_{1-x}Mn_xTe$ were indeed in accordance with these predictions (Bastard *et al.*, 1978; Jaczynski *et al.*, 1978). However, the g-factors, as determined experimentally, turned out to be much greater (easily by a factor of 2) than these expectations and, moreover, they depend rather strongly on the temperature. Clearly, the band structure model was inadequate to account for these observations.

The fact that only the spin properties seemed to be anomalous immediately suggested that the interaction with localized moments of Mn ions involving conduction electron spin is the source of the problem. As mentioned in Part II of this chapter, it is possible to represent this interaction by the Heisenberg-like Hamiltonian $H_{sd} = \sum_j J(\mathbf{r} - \mathbf{R}_j)\mathbf{s} \cdot \mathbf{S}_j$, with $\mathbf{S}_j$ and $\mathbf{s}$ standing for spin operators of the j-th Mn ion and the band electron, respectively. Calculating the matrix elements of H_{sd} with the basis functions, Eq. (10), one obtains an additional matrix which must be added to Eq. (11) before the eigenvalues of our problem are found:

$$D' = \frac{1}{N_0} \sum_j \begin{bmatrix} D'_a & D'_c \\ D'^{\dagger}_c & D'_b \end{bmatrix}, \tag{22}$$

where

$$D'_a = \begin{bmatrix} \frac{1}{2}\alpha S_{z_j} & 0 & 0 & 0 \\ 0 & \frac{1}{2}\beta S_{z_j} & 0 & 0 \\ 0 & 0 & -\frac{1}{6}\beta S_{z_j} & -\frac{i\sqrt{2}}{3} S_{z_j} \\ 0 & 0 & \frac{i\sqrt{2}}{3} S_{z_j} & \frac{1}{6}\beta S_{z_j} \end{bmatrix}, \tag{23}$$

$$D'_b = -(D'_a)^* \tag{24}$$

$$D_c' = \begin{bmatrix} \frac{1}{2}\alpha S_j^- & 0 & 0 & 0 \\ 0 & 0 & \frac{i}{2\sqrt{3}}\beta S_j^- & \frac{1}{\sqrt{6}}\beta S_j^- \\ 0 & \frac{\beta}{2\sqrt{3}} S_j^- & \frac{1}{3}\beta S_j^+ & \frac{\sqrt{2}}{6}\beta S_j^- \\ 0 & -\frac{1}{\sqrt{6}}\beta S_j^- & \frac{i\sqrt{2}}{3}\beta S_j^+ & -\frac{1}{6}\beta S_j^+ \end{bmatrix}, \tag{25}$$

where $S_j^{\pm} = S_j^x \pm iS_j^y$ and, as in Part II, the only nonvanishing and independent exchange constants are defined as

$$\alpha = \frac{1}{\Omega_0}\langle S|J|S\rangle \tag{26}$$

$$\beta = \frac{1}{\Omega_0}\langle X|J|X\rangle = \frac{1}{\Omega_0}\langle Y|J|Y\rangle = \frac{1}{\Omega_0}\langle Z|J|Z\rangle. \tag{27}$$

Here Ω_0 is the unit cell volume, and $N_0 = V/\Omega_0$ is the number of cation sublattice sites.

The matrix (22) is of rather complex form. The problem is further complicated by the fact that after addition of (22) to (11), its solutions can no longer be sought as a simple vector-column of harmonic oscillator eigenfunctions. The matrix (22) can be, however, considerably simplified when an approximation analogous to the mean field approximation from the physics of magnetism is invoked. Namely, the wave functions of conduction and valence band electrons are spread over the whole volume of the crystal. Therefore, one may say that these electrons interact with all magnetic moments present in a sample, thus "feeling" in effect the average value of the localized moments. One may thus say that the band electrons are subject to a certain average or resultant field of the localized moments. It is therefore permissible to carry out an averaging procedure over all possible states of Mn moments already at the level of the Hamiltonian matrix. For a paramagnetic system only the S_z component of the localized spin does not vanish after the averaging procedure. This very major approximation was confirmed *a posteriori* by Gaj *et al.* (1979) who determined experimentally a direct proportionality between spin splittings and magnetization that is proportional to $\langle S_z\rangle x$ (note that $\sum_j \langle S_{zj}\rangle/N_0 = x\langle S_z\rangle$).

After this averaging procedure the entire off-diagonal blocks D_c' in Eq. (22) vanish and one is left with two nearly diagonal 4×4 blocks D_a' and D_b'. The matrix resulting from the addition of Eq. (11) and Eq. (22), with D_c' blocks

omitted, may then be solved in terms of the harmonic oscillator wavefunctions.

The new parameters α and β are treated as adjustable parameters (their fitted values are discussed further in this chapter). The values of $\langle S_z \rangle$ which depend on the crystal composition and also on the temperature and magnetic field strength are either calculated assuming some simple model (see, e.g., Galazka and Kossut, 1980) or taken from an independent experiment measuring the magnetization of the samples.

An example of the diagonalization is shown in Fig. 3, where a series of the conduction and heavy hole Landau levels is shown for zero-gap $Hg_{1-x}Mn_xTe$ at two temperatures. The strong temperature dependence of the band structure occurs via the terms involving $\langle S_z \rangle$. While the band structure at $T = 30$ K (Fig. 3b) resembles that of nonmagnetic $Hg_{1-x}Cd_xTe$ with corresponding energy gap, the situation at low temperatures $T = 1.4$ K in Fig. 3a is qualitatively different. We shall enumerate the most important of these differences below.

Ordering of the Landau Levels

The first thing to be noted in Fig. 3 is an enhancement of the low temperature spin splitting (marked by thick solid arrows), which was achieved by putting a positive value of β. As we pointed out earlier, such an enhancement was indeed observed experimentally. Note also that the higher of the spin-split Landau levels (*b*-set levels) are shifted so strongly upwards in low temperature that they cross the Landau levels from the *a*-set of solutions with a greater harmonic oscillator quantum number n.

This feature constitutes a unique attribute of narrow-gap DMS: the spin splitting, being ruled mainly by the exchange interaction of the band carriers with the localized magnetic moments, may easily exceed the cyclotron splitting that is due to the effect of the external magnetic field on the orbital degrees of freedom of an electron or a hole. This is particularly true in the case of the heavy holes for which the cyclotron splitting is rather small because of the large value of their effective mass. Therefore, DMS may be viewed as systems where "amplification of the spin properties" takes place. The degree of this amplification is, furthermore, tunable by the temperature.

Conduction and Valence Band Overlap

A second striking feature to be noted in Fig. 3 is the existence of the band overlap at low temperature. The presence of strong magnetic field lifts the degeneracy of the conduction and heavy hole bands in zero-gap semiconductors. In diluted magnetic semiconductors, the uppermost heavy hole subband (indicated by an arrow in Fig. 3) is shifted upwards, contrary to the case of, e.g., $Hg_{1-x}Cd_xTe$ where this shift is directed downwards so that a

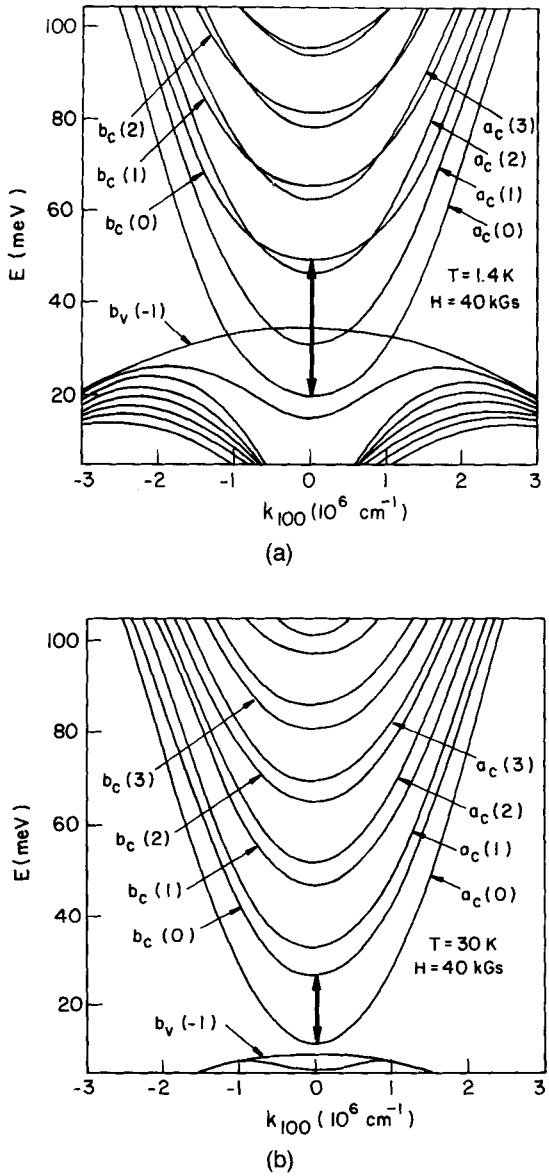

FIG. 3. The Landau subband energies in $Hg_{1-x}Mn_xTe$, $x = 0.025$ calculated at a constant magnetic field and at (a) $T = 1.4$ K and (b) $T = 30$ K as a function of the wave vector k_H along the magnetic field direction. The field is applied along the ⟨100⟩ crystallographic axis. Thick vertical arrows indicate spin splitting of the lowest conduction-band Landau level. The valence band Landau level $b_v(-1)$ is indicated by thin arrow. [After Dobrowolska *et al.* (1979); reprinted with permission of Pergamon Press, Ltd.]

real energy gap opens. Therefore, it may happen that the band gap in DMS opens only at elevated temperatures.

The magnitude of the band overlap is a result of an interplay between this exchange interaction-induced shift and the movement of the lowest conduction band that occurs also in the upward direction on the energetic scale. For very small values of E_g (close to the semimetal–semiconductor transition), the conduction band levels (due to the smallness of their effective mass) move up faster than the top of the valence band, and the overlap may not occur even at very low temperature. Also, for sufficiently high magnetic fields the shift of the top of the valence band reverses its sign and the level beings to move downwards, as it does in standard narrow-gap semiconductors. Then the energy gap induced by the field starts to open.

This strange behavior of the top of the valence band may be qualitatively understood when one bears in mind how $\langle S_z \rangle$ depends on the temperature and magnetic field. Let us assume for a moment that we are dealing with a perfect paramagnet where the magnetic moments do not interact with each other. Then $\langle S_z \rangle$ varies as $1/T$, so that at higher temperatures the additional terms proportional to $\langle S_z \rangle$ may become negligible compared to "normal" terms brought by Eq. (11). The magnetic field tends to align the magnetic moments along its direction. When all the moments are already aligned a saturation is reached and $\langle S_z \rangle = -5/2$. The "normal" terms in Eq. (11), on the other hand, are directly proportional to the field. A value of the magnetic field may thus be reached when the contribution of these normal terms wins over the exchange induced contribution. For the top of the valence band such a return to "normalcy" occurs if the following condition is met:

$$\frac{\hbar eH}{m_0 c}\left[\frac{1}{2}\gamma_1 + \gamma_2 + \frac{3}{2}\kappa\right] > \frac{1}{2}x\beta\langle S_z \rangle. \tag{28}$$

The above general remarks remain true even if the interaction between the localized moments becomes appreciable and $\langle S_z \rangle$ cannot be described by a simple Brillouin function applicable to non-interacting spin systems.

Shape of the Heavy Hole Landau Levels

Another feature in which diluted magnetic semiconductors differ from their nonmagnetic counterparts, is existence of very pronounced "camel backs" in the heavy hole Landau levels with large quantum number n. Such a "camel back" shape of the heavy hole Landau subbands is characteristic also for ordinary narrow-gap semiconductors. However, in diluted magnetic semiconductors it is particularly large at low temperatures. Since this shape is enhanced by the $\langle S_z \rangle$ terms, the magnitude of the "camel backs" decreases with the temperature, as can be seen in Fig. 3.

Reduction of the g-Factor above the Semimetal-to-Semiconductor Transition

Finally, let us turn our attention to the region "open-gap" of diluted magnetic semiconductors, i.e., to compositions above the semimetal-semiconductor transition (that occurs, e.g., at $x = 0.065$ in $Hg_{1-x}Mn_xTe$ at 4.2 K). The conduction band is then of Γ_6 symmetry and the electronic wave functions are mainly of s-like character. Therefore, one may expect that the modifications of the band structure due to the s-d interaction will be mainly described by the constant α. The sign of α (determined experimentally) is in our notation negative, i.e., opposite to the sign of β. Therefore, the exchange contribution to the electronic g-factor in the open-gap DMS is also opposite in sign to that contribution in zero-gap DMS. Since the exchange induced contributions in both zero-gap and open-gap narrow gap DMS constitute a sizable part of the total spin splitting of the conduction electrons, one can, consequently, expect a reduction of the electronic spin splitting at very low temperature in the latter. The absolute value of α is found to be smaller than that of β, thus this reduction is expected to be less pronounced than the enhancement observed in the case of zero-gap materials. Figure 4

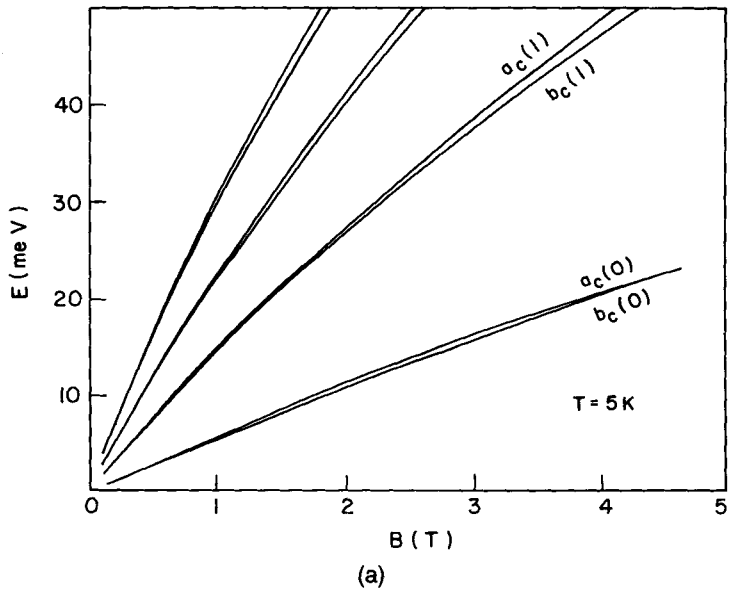

FIG. 4. The energies of the minima of the conduction subbands ($k_H = 0$) in $Hg_{1-x}Mn_xTe$ ($x = 0.1$), calculated at (a) $T = 5$ K, (b) $T = 15$ K and (c) without the contribution of the exchange interaction (i.e., for $\alpha = \beta = 0$) as a function of an external magnetic field.

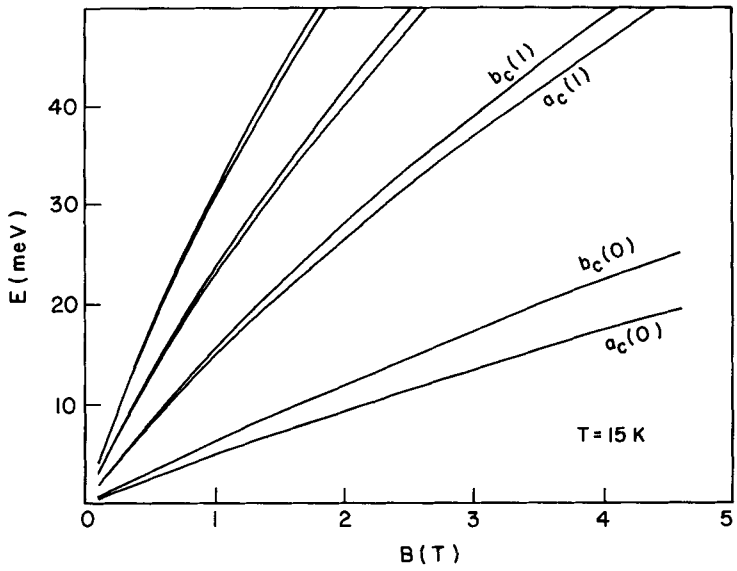

(b)

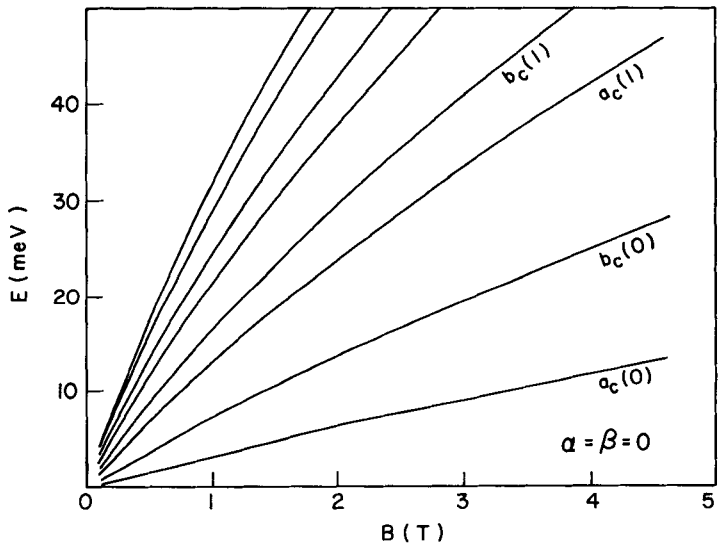

(c)

FIG. 4 (*continued*)

presents results of numerical diagonalization of matrices (11) and (22) for $Hg_{1-x}Mn_xTe$ with $x = 0.1$. Only the minima of the conduction band Landau levels ($k_z = 0$) are shown. For the sake of comparison, the Landau levels in the "nonmagnetic" counterpart (the same band parameters, but for $\alpha = \beta = 0$) are given in Fig. 4c.

One may observe that the spin splitting is indeed greatly reduced. For $T = 5$ K, even the level ordering is opposite, which corresponds to a very small but positive value of the g-factor. So, there is again a qualitative difference with non-magnetic narrow-gap semiconductors where the g-factors determined mainly by the spin–orbit interaction are generally negative. The positive g-factors—and their sign reversal with increasing temperature— have been, in fact, observed experimentally in the magneto-optical experiments (see Rigaux, this volume).

IV. Transport Measurements in the Quantum Regime: Confirmation of the Band Structure Model

The study of transport phenomena in strong quantizing magnetic fields (in particular, the Shubnikov-de Haas effect) is a useful tool of investigating the band structure. Since the Landau quantization is strong in semiconductors with small effective masses, the method is particularly well suited for narrow-gap semiconductors. In the present section, we shall describe the experimental data on the quantum transport phenomena, stressing these aspects that reflect the unique band structure character of diluted magnetic semiconductors. The sequence of the sections will be the following: first we shall focus our attention on the zinc blende materials $Hg_{1-x}Mn_xTe$ and $Hg_{1-x}Mn_xSe$, for which the greatest amount of data is available. Next we proceed to tetragonal DMS and lead salts containing manganese (e.g., $(Cd_{1-x}Mn_x)_3As_2$ and $Pb_{1-x}Mn_xTe$), which are only at the initial stages of investigation. Our attention throughout this section will be limited to n-type samples. We will thus, not discuss in this chapter the experiments on the quantum transport phenomena in p-type samples of zero-gap $Hg_{1-x}Mn_xTe$ (see, e.g., Sawicki *et al.*, 1982 and Ponikarov *et al.*, 1981). The peculiarities observed in these samples are mainly associated with the pinning of the Fermi level by the acceptor states degenerate with the conduction band.

3. $Hg_{1-x}Mn_xTe$ AND $Hg_{1-x}Mn_xSe$

The quantum transport study of $Hg_{1-x}Mn_xTe$ by Morrissy (1973) was the first to reveal anomalies, characteristic for what later become known as semimagnetic or diluted magnetic semiconductors. However, the anomalies remained largely unexplained until the band structure model as described in Section III was developed by Bastard *et al.* (1978) and Jaczynski *et al.* (1978).

Further in this section we shall try to describe the most striking differences between the quantum transport phenomena observed in diluted magnetic and nonmagnetic semiconductors, and we shall discuss how the anomalies occurring in DMS can be understood.

a. Temperature Dependence on the Shubnikov-de Haas Peak Positions

The magnetic field positions of the maxima (or minima) observed in the Shubnikov-de Haas (SdH) effect are mainly determined by the crossing of the Fermi level with consecutive Landau levels. Their temperature dependence is, in usual materials, only very slight. It was, therefore, quite surprising to observe a very strong temperature shift of the maxima of the SdH effect in $Hg_{1-x}Mn_xTe$ (Jaczynski *et al.*, 1978). The shift was particularly pronounced in the case of the spin split peaks. The small temperature variation of the effective mass of conduction electrons could not possibly account for the observed shifts.

These shifts are quite naturally explained in terms of the band structure model incorporating the s-d exchange terms presented in Section III of this chapter. They are due to a strong temperature dependence of the terms proportional to $\langle S_z \rangle$, that govern the spin splittings of the Landau levels, and also, but to a much lesser degree modify the positions of the unsplit Landau levels. Similar strong temperature dependence was also observed in later Shubnikov-de Haas effect studies both in $Hg_{1-x}Mn_xTe$ by Byszewski *et al.* (1979) and $Hg_{1-x}Mn_xSe$ by Takeyama and Galazka (1979), Byszewski *et al.* (1980) and Lyapilin *et al.* (1983).

It should be mentioned that in the case of the very last oscillation, i.e., that occurring at the highest magnetic field (often labeled 0^-), the Shubnikov-de Haas peak exhibits a relatively strong dependence on the temperature also in nonmagnetic semiconductors. This has its source in the partial lifting of a strong degeneracy of the electron gas. However, in diluted magnetic semiconductors, as noted in $Hg_{1-x}Mn_xSe$ by Lyapilin *et al.* (1983), the 0^- peak observed in intense magnetic fields may shift towards smaller fields when the temperature is increased. This is exactly the opposite direction of the temperature shift of the 0^- peak to that observed in nonmagnetic semiconductors. Hence, the usual explanation may again not be applied to the case of diluted magnetic semiconductors. On the other hand, both the direction of the 0^- shift and its magnitude can be readily explained by the variation of the Landau level ($n = 0$, set b) with temperature due to the exchange terms proportional to $\langle S_z \rangle$.

Probably the most striking feature in the SdH behavior of DMS was the evolution the temperature of a well resolved doublet structure of Shubnikov-de Haas peaks that remained unsplit at lower temperatures. This can be clearly seen in Fig. 5 in the case of the oscillation maxima associated with

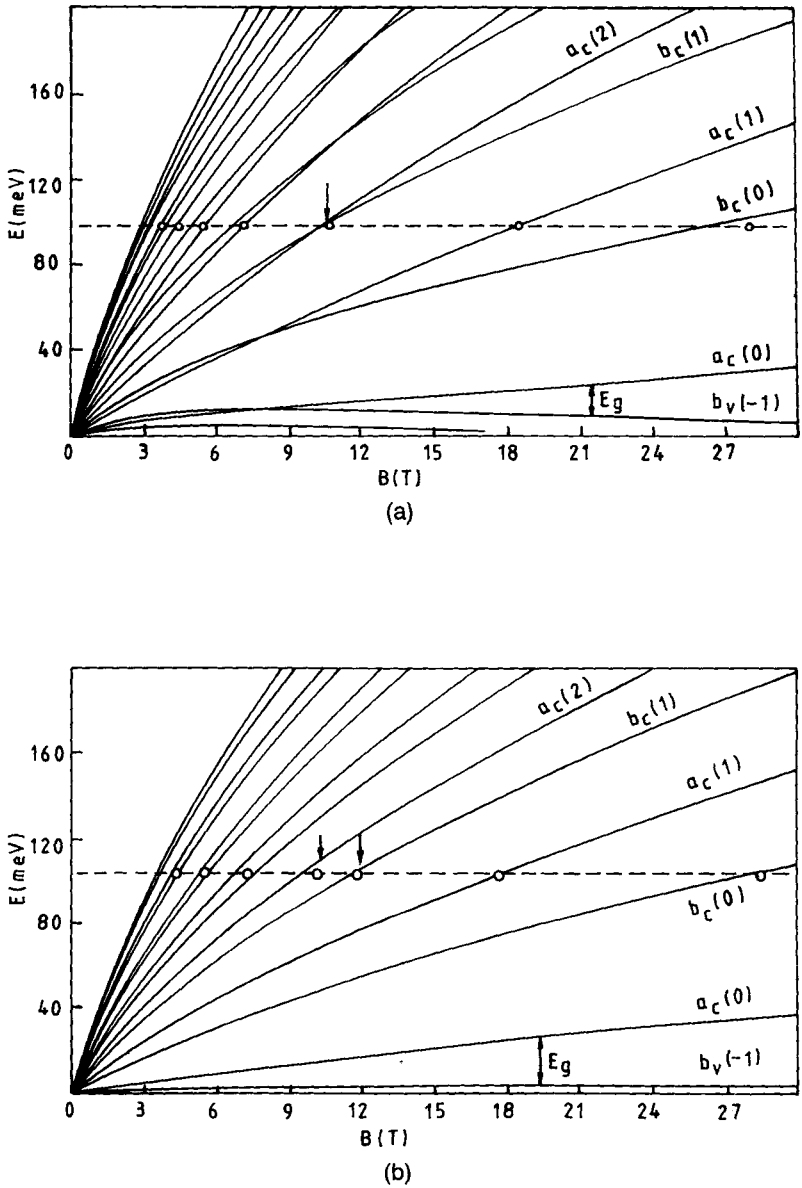

FIG. 5. The Landau levels at $k_H = 0$ in $Hg_{1-x}Mn_xTe$ ($x = 0.02$) calculated at (a) $T = 4$ K and (b) $T = 36$ K using the value of $\beta = 0.6$ eV and $\alpha = -0.4$ eV. Open circles show the positions of the maxima of the Shubnikov-de Haas oscillations observed by Byszewski *et al.* (1979). Arrows indicate the peak which splits at elevated temperatures. Note that at the lower temperature the energy gap opens only above $8T$.

a_c (2) and b_c (1) Landau levels—sometimes labeled as 2^+ and 1^- levels—in $Hg_{1-x}Mn_xTe$ ($x = 0.02$). This is contrary to the case of nonmagnetic semiconductors where the increase of the temperature leads usually to a smearing out of the observed maxima. Again, this anomalous feature is naturally accounted for by the exchange-induced modifications of the band structure. The spin-splitting at the lower temperature is so big that the b_c (1) spin-split Landau level nearly coincides with the a_c (2) level. Thus, a single Shubnikov-de Haas maximum is observed. When the temperature is raised, the value of $\langle S_z \rangle$ and, thus the spin splitting is reduced. Consequently, the b_c (1) sublevel is sufficiently separated from the a_c (2) sublevel for the doublet structure to appear. Similar behavior was also observed in the case of $Hg_{1-x}Mn_xSe$ crystals by Lyapilin *et al.* (1983).

The temperature dependence of the Shubnikov-de Haas maxima provides an abundance of information that, in principle, enables a precise determination of the band structure parameters. The analysis aimed at such determination requires, however, a detailed knowledge of the $\langle S_z \rangle$, particularly of its dependence on the temperature, composition x and magnetic field. This can be obtained independently from the measurements of the magnetization. Lack of reliable measurements of this quantity made the interpretation of SdH data rather difficult, and led to inaccuracies of the values of the band structure parameters determined at the initial stages of research on $Hg_{1-x}Mn_xTe$ and $Hg_{1-x}Mn_xSe$. We shall return to this problem later in this section.

b. Thermo-Oscillations

The strong temperature dependence of the energies at which the Landau levels occur suggests that at a constant magnetic field (that provides the Landau quantization), the temperature sweep will cause the crossing of various Landau levels with the Fermi energy, if the carrier concentration in a sample is properly chosen. These crossings will then lead to successive peaks in the magneto-resistivity of the sample observed as a function of temperature, similar to those observed by sweeping the magnetic field at a constant temperature in the usual Shubnikov-de Haas experiment. Such peaks in the resistivity were observed in $Hg_{1-x}Mn_xTe$ by Dobrowolska *et al.* (1979) as shown in Fig. 6. The phenomenon was named the thermo-oscillation of magnetoresistance. An experiment similar in nature but involving the oscillations of the absorption of sound was suggested theoretically by Lyapilin and Karyagin (1980).

Although the thermo-oscillations are difficult to interpret quantitatively, they serve to illustrate rather dramatically the unique temperature dependence of the Landau quantization of DMS owing to the contributions associated with the magnetization in these materials.

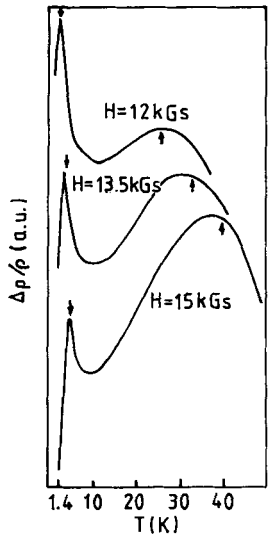

FIG. 6. Resistivity in $Hg_{1-x}Mn_xTe$ ($x = 0.009$) versus temperature showing thermo-oscillation maxima. The arrows indicate the theoretically expected positions of the maxima. [After Dobrowolska *et al.* (1979).]

c. The Amplitude of the Shubnikov-de Haas Oscillations

The temperature dependence of the amplitude of the magnetoresistance oscillations is an important feature of the Shubnikov-de Haas effect, since it provides a source of information concerning the electron effective mass at the Fermi level. Usually, in nonmagnetic semiconductors, the amplitude of a given magnetoresistance maximum decreases monotonically when the temperature is increased. It was therefore quite surprising to observe (Jaczynski *et al.*, 1978) that in $Hg_{1-x}Mn_xTe$, the amplitude behaved in a drastically non-monotonic manner (see Fig. 7). It dropped quickly with increasing temperature, passed a region of very small values where the oscillations were hardly detectable, and became appreciable once again at even higher temperatures. Then, after passing through a maximum, it started to decrease again. Only the last portion of this behavior, in the highest temperature range, could be consistently understood in terms of the theory usually applicable to nonmagnetic semiconductors. A very similar temperature dependence of the Shubnikov-de Haas amplitude was observed in $Hg_{1-x}Mn_xSe$ (Takeyama and Galazka, 1979; Lyapilin *et al.*, 1983).

The theory of the Shubnikov-de Haas effect (see, e.g., Roth and Argyres, 1966) gives the following expression, conveniently expressed in the form of

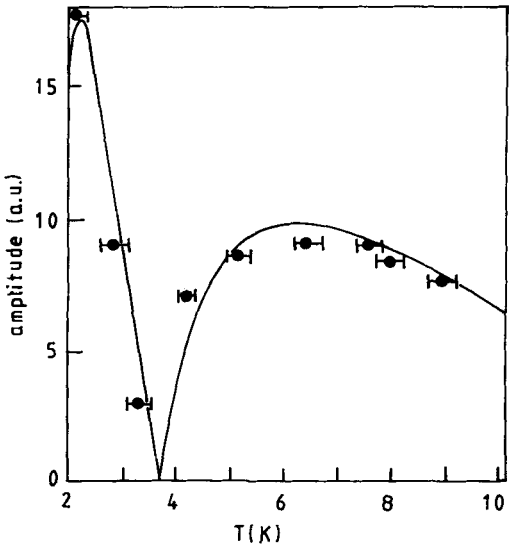

FIG. 7. The amplitude of the Shubnikov-de Haas oscillation in $Hg_{1-x}Mn_xTe$ ($x = 0.02$) as a function of temperature. The solid line is calculated using the temperature-dependent g-factor. [After Jaczynski *et al.* (1978).]

a harmonic series, for the amplitude behavior of the SdH oscillations:

$$\frac{\Delta\rho}{\rho_0} \sim \sum_{r=1}^{\infty} \frac{\sqrt{H}X_r \exp(-arT_D/H)}{\sqrt{r}\sinh X_r} \cos(\pi\nu r) \cos\left[2\pi r\left(\frac{P_{SH}}{H} - \gamma\right) \pm \frac{\pi}{4}\right] \quad (29)$$

where $a = 2\pi^2 m^* k_B/e\hbar$, T_D is the Dingle temperature describing phenomenologically the broadening of the Landau levels, $X_r = arT/H$, ν is the spin splitting factor defined as

$$\nu = \frac{1}{2} g^* \frac{m^*}{m_0},$$

with m^* and m_0 standing for, respectively, the effective mass and the free electron mass. The oscillatory character of the magnetoresistance is given by the last cosine factor in Eq. (29) with the fundamental period P_{SH}. For spherical Fermi surfaces, this can be related to the electron concentration N by

$$P_{SH} = \frac{1}{2} \frac{\hbar c}{e} (3\pi^2 N)^{2/3}.$$

Often only the first few terms of the expansion (29) are of importance, because of the exponential damping factor involving T_D. The temperature

behavior of the amplitude is given by the factor $X_r/\sinh X_r$ in Eq. (29), provided that there is no implicit temperature dependence of the remaining coefficients in Eq. (29). Now, in a diluted magnetic semiconductor, as we have pointed out in the previous sections, the temperature dependence of the g-factor can be quite remarkable, and thus the $\cos(\pi\nu r)$ term in Eq. (29) can influence the temperature behavior of the amplitude quite significantly. When the argument of the cosine is equal to $i\pi/2$, where i is an odd integer, the amplitude may vanish. For the first harmonic in Eq. (29), i.e., for $r = 1$, the condition for the zeros can be written explicitly as

$$g^* = \frac{m_0}{m^*} i; \qquad i = \pm 1, \pm 3. \tag{30}$$

When the g-factors given by the band structure calculation for $Hg_{1-x}Mn_xTe$ were calculated, it turned out that, indeed, it is possible to meet condition (30) in the temperature range where the Shubnikov-de Haas effect was studied. A superposition of the factors $X_1/\sinh X_1$ and $\cos(\pi\nu)$ gave a good description of the amplitude vs. temperature curve (see the solid line in Fig. 7). The condition (30) suggests, further, that more than one zero of the amplitude can be expected as a function of the temperature. In fact, two zeros were detected in $Hg_{1-x}Mn_xSe$ by Lyapilin *et al.* (1983). The temperatures at which both amplitude zeros occurred could be well accounted for by the simple explanation presented above.

Let us note that condition (30) corresponds to the situation where the Landau spin-split sublevels are equally spaced in energy. This is an easy situation for the collision broadening of the levels to smear out the quantum oscillations, i.e., to produce a zero of the amplitude. So, one expects an occurrence of a clear zero in relatively impure samples with rather high values of the Dingle temperature T_D. Such values enable one to neglect all higher terms in the harmonic series, Eq. (29). For purer samples, when more terms in the harmonic expansion are important, only a minimum of the amplitude vs. temperature relationship can be expected (Kossut, 1978).

The analysis of the positions of the zeros of the amplitude as a function of temperature can serve as a rather precise method for determining the g-factor, as well as the exchange constants α and β. This method was actually employed in the case of $(Cd_{1-x}Mn_x)_3As_2$ mixed crystals (see further in this part).

Recently, Reifenberger and Schwarzkopf (1983) have suggested a different explanation for the beating of the amplitude of the Shubnikov-de Haas effect observed by them in $Hg_{1-x}Mn_xSe$ with small x and also in HgSe at weak magnetic fields. They suggest that the beating effect, which can be interpreted as a zero of the amplitude at a certain magnetic field, is due to

the magnetic breakdown between the closed-orbits in the spin-split conduction band. The splitting results from the lack of inversion symmetry characteristic for the zinc blende lattice structure. Actually, the fact that the beating effect is also found by Reifenberger and Schwarzkopf (1983) in HgSe leads them to reject the explanation in terms of the $\cos(\pi\nu)$ factor described above. In order to account for the temperature shift of the beat fields observed in $Hg_{1-x}Mn_xSe$ samples, Reifenberger and Schwarzkopf (1983) conclude that substitution of Mn for Hg atoms makes the linear k terms in the $\mathbf{k} \cdot \mathbf{p}$ Hamiltonian also sensitive to the temperature in this material.

d. Conduction and Valence Band Overlap

The degeneracy of the conduction and heavy hole valence band edges in zero-gap HgTe and $Hg_{1-x}Cd_xTe$ is lifted when the magnetic field is applied and a real energy gap, induced by the field, opens. As we have seen in Part III of this chapter, the situation in semimagnetic $Hg_{1-x}Mn_xTe$ and $Hg_{1-x}Mn_xSe$ is quite different. The degeneracy of the Γ_8 level is, of course, also lifted, but in these DMS a strong upward shift of the uppermost Landau level of the heavy hole band may result in an overlap of the bands (see Fig. 5a). The extent of the overlap can be calculated analytically and is given by,

$$\begin{aligned}\Delta E &= E_{b_v(-1)} - E_{a_c(0)} \\ &= x\langle S_z\rangle\left[\frac{\alpha}{4} + \frac{5\beta}{12}\right] - \frac{E_g}{2} + \frac{\hbar eH}{2m_0c}(2\gamma_1 - 4\gamma_2 + 2\kappa - F - 1) \\ &\quad - \frac{1}{2}\left\{\left[E_g + \frac{\hbar eH}{m_0c}\left(F + 1 + \frac{3}{2}\gamma_1 - \frac{3}{2}\gamma_2 - \frac{1}{2}\kappa\right)\right.\right. \\ &\quad \left.\left. + \frac{1}{2}x\langle S_z\rangle\left(\alpha + \frac{\beta}{3}\right)\right]^2 + \frac{4eH}{3\hbar c}P^2\right\}^{1/2}, \end{aligned} \tag{31}$$

where we assumed that $\Delta = \infty$.

The overlap corresponds to a positive ΔE, while for an open gap the value of ΔE is negative. The value of the band overlap is a resultant of several factors. First there is an upward movement of the lowest conduction band level $a_c(0)$ with the magnetic field, determined mainly by the effective mass (or, more precisely, by the cyclotron frequency) characterizing the conduction band. The variation of this level with the magnetic field is modified by exchange interaction to a lesser degree by the exchange interaction than that of the uppermost valence band Landau level $b_v(-1)$. The latter level, whose energy in nonmagnetic semiconductor decreases with increasing magnetic field, may be shifted in DMS to considerably higher energies if the

following condition is fulfilled:

$$\frac{1}{2}x\beta\langle S_z\rangle > \frac{\hbar eH}{m_0 c}\left[\frac{1}{2}(\gamma_1 + \gamma_2) + \frac{3}{2}\kappa\right] \tag{32}$$

Since $\langle S_z\rangle$ has a tendency to saturate in the magnetic field while the right hand side of Eq. (32) is linear in the field, the above condition can only be met in relatively small field region, if at all. Of course, the lower the temperature, the easier it is to satisfy the inequality (32). Because of antiferromagnetic interactions between the localized magnetic moments in $Hg_{1-x}Mn_xTe$ and $Hg_{1-x}Mn_xSe$, the value of $x\langle S_z\rangle$ at a given field and temperature is a decreasing function of x for samples with the Mn mole fraction greater than $x \approx 0.05$. At the same time, the rate at which the $a_c(0)$ level moves up in energy with the field increases with x in zero-gap materials, because the effective mass at the bottom of the conduction band becomes smaller. Therefore, the existence of the overlap is limited to rather low Mn contents region. It is estimated that in both $Hg_{1-x}Mn_xSe$ and $Hg_{1-x}Mn_xTe$, the highest value of x for which the overlap may be observable is about 0.04–0.05.

The detailed knowledge of the magnetization (i.e., of $x\langle S_z\rangle$) is of course, quite crucial for this estimate. The use of values of $x\langle S_z\rangle$ taken from more or less substantiated theoretical models of magnetization can lead to an overestimation of the extent of the overlap.

The existence of the band overlap may lead to a substantial redistribution of carriers between the two bands in question. This, in turn, is reflected as an anomaly of various transport coefficients in very pure samples. In fact, the analysis of the conductivity tensor components by Sandauer and Byszewski (1982) gave the first direct evidence for the band overlap. It was found that the warping asymmetry of the heavy hole band, proportional to $\gamma_2-\gamma_3$, is also observable as the anisotropy of the band overlap in $Hg_{1-x}Mn_xTe$ (Sandauer *et al.*, 1983).

e. Spin Dependent Scattering

The presence of localized magnetic moments not only modifies the band structure of diluted magnetic semiconductors, but also gives rise to an additional scattering mechanism of the carriers. The contribution of this mechanism is not easy to observe experimentally, because it is quite difficult to separate it from the contributions of other, often more important, scattering mechanisms. Recently, existence of spin dependent scattering has been evidenced in $Hg_{1-x}Mn_xTe$ under quantum-limit conditions by Wittlin *et al.* (1980a). In their experiment, the sample was placed in a strong magnetic field, such that only the lowest conduction band level was occupied. The field

also caused a total alignment of the localized Mn spins, i.e., the region of saturation $\langle S_z \rangle = -\frac{5}{2}$ was reached. The sample was then illuminated by a microwave radiation with energy chosen in such a way that it correponded to the condition of electron paramagnetic resonance of the Mn-subsystem. The resonant absorption by the Mn ions and the change of the polarization of the localized moments associated with it were visible as an increase of the resistivity of the sample. The possibility of other mechanisms (e.g., bolometric effect, influence of the optical excitation of the carriers between the Landau levels, etc.) contributing to the observed increase was ruled out by the authors. On the other hand, when the resistivity change connected with the sudden variation of the spin dependent scattering at the resonance condition is calculated (Wittlin *et al.*, 1980b), the correct magnitude of the observed effect is obtained.

f. Values of Exchange Constants Obtained from Quantum Transport Measurements

The results of the early studies of the Shubnikov-de Haas effect in $Hg_{1-x}Mn_xTe$ by Jaczynski *et al.* (1978) led to rather high values of the exchange constants: $\beta = 1.4$ eV and $\alpha = -0.7$ eV. These values were in agreement with the original results of magnetooptical measurements of Bastard *et al.* (1978). However, it must be stressed that in both studies, the magnetization of the investigated samples was, in fact, unknown. Moreover, the interpretation of the Shubnikov-de Haas oscillation pattern (Jaczynski *et al.*, 1978) assumed that the Fermi level remained constant in the entire range of magnetic fields investigated. This may be a good approximation when many Landau levels are below the Fermi level E_F, but becomes doubtful in higher fields, when only few Landau levels remain below E_F. Unfortunately, this is exactly the region of fields where the spin splitting of the SdH maxima was resolved, that is, where the subsequent analysis was sensitive to the choice of α and β. Substantial error could therefore be present in the determination of α and β by Jaczynski *et al.* (1978). Later investigations of the Shubnikov-de Haas effect (Sandauer and Byszewski, 1982), free of the two above mentioned approximations, put the value of $\beta = 0.8$–0.9 eV and $\alpha = -0.3$ eV. These values are considerably smaller than those originally proposed and are much closer to $\beta = 0.6$ eV, $\alpha = -0.4$ as determined from intraband (Pastor *et al.*, 1979) and interband (Dobrowolska and Dobrowolski, 1981) magneto-absorption.

A similar situation is also true for $Hg_{1-x}Mn_xSe$. The investigation of the material by Takeyama and Galazka (1979) yielded values of $\beta = 1.4$ eV and $\alpha = -0.9$ eV for $x = 0.01$ and $x = 0.016$, while for the $x = 0.066$ sample, $\beta = 0.9$ eV and $\alpha = 0.3$ eV. Later, when the magnetization of the samples was studied as well, it was found that the observed spin splitting is described

by $\beta = 0.9$ eV and $\alpha = -0.35$ eV (Byszewski *et al.*, 1980). Again, these later values are in better agreement with the magnetooptical determination of Dobrowolska *et al.* (1981) where $\beta = 0.7$ eV and $\alpha = -0.4$ eV.

Recently, Lyapilin *et al.* (1983) found, by an analysis of the spin splitting of the $n = 1$ Landau level observed in the Shubnikov–de Haas experiments in $Hg_{1-x}Mn_xSe$, that the value of β is still smaller: $\beta = 0.28$ eV. However, in their analysis Lyapilin *et al.* (1983) again did not use experimental values of magnetization, and, moreover, they employed a simplified band structure model.

Although there seems to be a trend toward reconciliation, the values of the exchange constants α and β in $Hg_{1-x}Mn_xTe$ and $Hg_{1-x}Mn_xSe$, as determined by various authors, do show a considerable disagreement. This is a situation distinctly different from that of wide gap DMS, where α and β are known with a greater accuracy. This unsatisfactory state of our knowledge is, at least partially, due to the complicated nature of the band structure of narrow gap DMS, where both spin and orbital quantization have to be simultaneously considered. Undoubtedly, this situation will be improved in a foreseeable future.

4. $(Cd_{1-x}Mn_x)_3As_2$

The very complex crystal structure of semiconducting Cd_3As_2 (symmetry C_{4v}^{12}) can be approximated fairly well by a cubic structure with an additional tetragonal distortion (see Kildal, 1974; Blom, 1980). Bodnar (1978) found that treating this distortion as a perturbation in the $\mathbf{k} \cdot \mathbf{p}$ scheme provides a reasonably good description of the band structure of the compounds in question. This model is a generalization of the three band approach to zinc blende semiconductors (Kacman and Zawadzki, 1971) in the sense that it takes similar basis functions into the quasi-degenerate set of states and neglects the effect of the higher bands entirely. The $\mathbf{k} \cdot \mathbf{p}$ perturbation Hamiltonian contains, as mentioned above, an additional parameter δ describing the axial distortion, that lifts the degeneracy of the conduction and heavy hole bands characteristic for the inverted band structure of zinc blende compounds. There appears a real—although small—energy gap. Of course, the presence of the axial crystal field leads to a strong anisotropy of the band structure noted by Wallace (1979).

The calculation of the Landau level in the presence of exchange interaction proceeds quite analogously to the method described in detail for zinc blende compounds in Section III of this chapter (Neve *et al.*, 1982). The main difference between the present case and previous calculations is that the tetragonal distortion introduces, instead of a single constant β describing the exchange interaction of p-like electrons with magnetic moments of Mn ions,

two such constants $\beta_\perp$ and $\beta_\parallel$ which, in general, may have different values. This fact may contribute additionally to the anisotropy of the g-factor of $(Cd_{1-x}Mn_x)_3As_2$.

Much less experimental information is available on this diluted magnetic semiconductor system than in the case of $Hg_{1-x}Mn_xTe$. The Shubnikov-de Haas effect was investigated in this material by Neve *et al.* (1981). Because of relatively high electron concentration in these crystals (of the order of $5 \times 10^{18}\,cm^{-3}$), it was impossible to determine the variation with x of such parameters as the energy gap and the momentum matrix elements $P_\perp, P_\parallel$ (again, because of the tetragonal distortion, the model contains two independent momentum matrix elements).

However, it was noted that the pattern of the oscillations was quite distinct from that in pure Cd_3As_2 crystals. In particular, the oscillations exhibited a strong beating effect, with the position of the nodes sensitive to temperature. When the amplitude at a fixed field was plotted versus the temperature, it was noted that two zeros were observed (see Fig. 8) that, when interpreted as being due to the $\cos(\pi\nu r)$ term (see subsection IV.3c of this chapter), rendered the values of the exchange constants $\beta_\perp = \beta_\parallel = 4.9\,eV$ and $\alpha = -3.4\,eV$. These values are remarkably greater than those in diluted magnetic semiconductors with the zinc blende lattice structure.

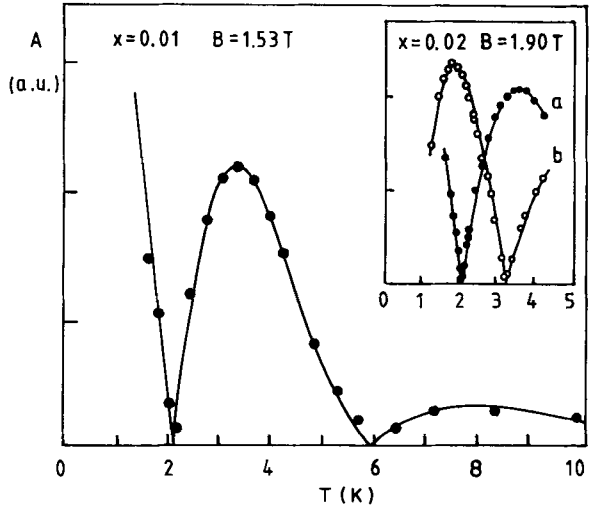

FIG. 8. Temperature dependence of the Shubnikov-de Haas amplitudes in $(Cd_{1-x}Mn_x)_3As_2$ ($x = 0.01$). The points represent experimental data, and the solid lines are fitted. In the insert the SdH amplitude vs. T curves are shown for two samples, both with $x = 0.02$ but differing in electron concentration: (a) $n = 3.9\,10^{18}\,cm^{-3}$ and (b) $n = 5.45\,10^{18}\,cm^{-3}$. [After Neve *et al.* (1981). Reprinted with permission of Pergamon Press Ltd.]

The anisotropy of the conduction band was also studied in $(Cd_{1-x}Mn_x)_3As_2$ by Blom *et al.* (1983) who studied the Shubnikov-de Haas effect in monocrystalline samples. The angular dependence of the effective mass was found to be qualitatively similar to that in Cd_3As_2. The anistropy of the g-factor was found to be smaller than predicted by a simple theory of Neve *et al.* (1982), and even less pronounced than in Cd_3As_2. This fact led Blom *et al.* (1983) to conclude that there must be a strong dependence of the energy gap E_g and the crystal field parameter δ on the crystal composition given by the Mn mole fraction x.

5. $Pb_{1-x}Mn_xTe$ AND $Pb_{1-x}Mn_xS$

In this section, we are dealing with diluted magnetic semiconductors based on lead chalcogenides, e.g., $Pb_{1-x}Mn_xTe$. These semiconductors crystalize in the NaCl cubic structure.

Again the calculation of the Landau levels in the presence of the exchange interaction can be done (within $\mathbf{k} \cdot \mathbf{p}$ approach) along the general lines given in Section III for zinc blende compounds (see, e.g., Niewodniczanska-Zawadzka, 1983). The calculation is however more complicated because of the anisotropic nature of the band structure of the host material, e.g., PbTe (Adler *et al.*, 1973). It is only for the magnetic field oriented along some special directions with respect to the crystallographic axes (e.g., $H \| \langle 111 \rangle$) that the problem is relatively easy to solve.

Preliminary investigation of the Shubnikov-de Haas effect in $Pb_{1-x}Mn_xTe$ by Niewodniczanska-Zawadzka *et al.* (1982) appeared to indicate that the presence of Mn ions modifies the band structure of this material in a manner predicted by the model outlined in Section III. A similar conclusion, although much more cautiously worded, was reached in the intraband magnetoabsorption study of Niewodniczanska-Zawadzka *et al.* (1983). The position of the magneto-absorption lines and of the Shubnikov-de Haas maxima in the recent study of Elsinger (1983) show practically no temperature dependence, contrary to strong temperature variation of the magnetization. In fact, these data can be interpreted in terms of the $\mathbf{k} \cdot \mathbf{p}$ theory disregarding the contribution of the exchange interaction. However, in order to explain the observed spectra, a large zero-field spin splitting of the valence band has to be assumed (Pascher *et al.*, 1983). It was found that the value of this splitting depends on the temperature.

A similar spin splitting at $H = 0$ was also discovered in the study of $Pb_{1-x}Mn_xS$ p–n junction lasers by Karczewski and Kowalczyk (1983). It is suspected that the off-diagonal terms involving the neglected components S_x and S_y of the localized moment are responsible for the zero-field splitting. It is still not clear why the influence of the terms proportional only to $\langle S_z \rangle$,

so pronounced in DMS with the zinc blende structure, is not observable in $Pb_{1-x}Mn_xTe$ and $Pb_{1-x}Mn_xS$. This may be related to the fact that the exchange constants for $Pb_{1-x}Mn_xTe$ are very small, as inferred by Toth and Leloup (1970), from the shape of the spin paramagnetic resonance line. The value found in this study (0.07 eV) is by an order of magnitude smaller than that characteristic of, e.g., $Hg_{1-x}Mn_xTe$. The question arises whether the lack of the splittings proportional to $\langle S_z \rangle$ is not related to the fact that the band edges in $Pb_{1-x}Mn_xTe$ and $Pb_{1-x}Mn_xS$ occur at the L point of the Brillouin zone. In $Cd_{1-x}Mn_xTe$ it was found (see Gaj, this volume) that there is a great reduction of such splittings at the L point, while at the zone center they are large and easy to observe. The solution to this problem requires further study.

V. Two-Dimensional Electron Gas in $Hg_{1-x}Mn_xTe$ and $Hg_{1-x-y}Cd_xMn_yTe$

The space charge layers in semiconductors have been intensively studied in recent years (see, e.g., review by Ando *et al.*, 1982). It was therefore natural to extend the studies of diluted magnetic semiconductors in this direction. So far, the inversion layers in p-$Hg_{1-x}Mn_xTe$ and a quaternary system $Hg_{1-x-y}Cd_xMn_yTe$ were investigated. These preliminary studies were performed by the quantum transport method and concerned the quasi two-dimensional electrons either on the surface of the semiconductor (Grabecki *et al.*, 1984a), or confined in a thin layer surrounding a grain boundary within the semiconductor (Grabecki *et al.*, 1984b). Here we shall discuss—after a very brief description of the experiments mentioned above—a simple model of the two-dimensional energy subbands that allows a semiquantitative interpretation of the data.

6. Experiments

In the first series of experiments by Grabecki *et al.* (1984a), the MIS structures were prepared by placing a thin sheet of Mylar as an insulator on the $Hg_{1-x}Mn_xTe$ surface. The p-type samples were used with the Mn mole fraction $x \approx 0.1$, that corresponded to an open energy gap of the order of about 100 meV (c.f., Fig. 2). The relatively high value of x was chosen to limit the effects of tunneling of electrons from the surface inversion layer to the valence band in the bulk of the crystal.

It was found that the conductivity at low temperatures is dominated by a flow of electrons within a thin quasi two-dimensional inversion layer produced by an attracting surface potential. This potential restricts the electronic motion in the direction perpendicular to the surface. The motion

in this direction becomes quantized: a series of surface or "electric" subbands is then produced. The electronic motion parallel to the surface remains unaffected in a first approximation. The concentration of the electrons in the inversion layer could be changed by means of an applied gate voltage.

When a sample is placed in a strong magnetic field and energy levels of electrons in the layer become further quantized (Landau quantization), an oscillatory structure in the conductivity vs. the gate voltage V_g curves can be recorded. Two periods of oscillation were detected, indicating that at least two surface subbands were populated by electrons. This observation reflects a small density of states of the conduction band in narrow-gap semiconductors related to the smallness of the effective mass.

By studying the ρ vs. V_g dependences at various temperatures, a remarkable shift of the resistivity maxima was noted. Two maxima that were clearly resolved at $T = 5$ K approached each other when the temperature was raised. At about 10 K only single maximum was observed, but at still higher temperature, about 14 K, a doublet structure became visible again. This effect was interpreted as being due a temperature shift of the Landau levels so characteristic for diluted magnetic semiconductors (see Section IV.3a of this chapter). However, it was possible to draw only rather qualitative conclusions from these preliminary experiments on the MIS structures. This was because of the rather low electrons mobilities in the inversion layers, reflecting severe problems with the proper preparation of the surfaces.

A more quantitative interpretation became possible quite recently when research began on a new quasi two-dimensional system of electrons. It was noted that the grain boundaries, often found in $Hg_{1-x}Mn_xTe$ crystals grown by the Bridgman method, can be a source of electronic confinement (Grabecki *et al.*, 1984b). Similar systems of two-dimensional electrons were already studied in Ge by Vul and Zavaritskaya (1979) and Uchida *et al.* (1983) (see also a review by Seager, 1982). The physical reason for the electron confinement is the presence of charge traps at the grain boundary. These may be associated with dislocations existing at the boundary, as is the case in Ge (Uchida *et al.*, 1983). The samples containing a single boundary plane (often referred to in the literature as bicrystals) were carefully cut out of a slice of $Hg_{1-x}Mn_xTe$ material with $x \approx 0.1$ where special etching techniques made the boundaries between monocrystalline grains visible.

It was found by Grabecki *et al.* (1984b) that, although the single grain samples prepared from the same ingot exhibited typical p-type behavior, the low temperature conductivity of samples containing the grain boundary was due to electrons. Further, it was also observed that these electrons possessed features of the quasi two-dimensional gas: the Landau quantization of their states depended only on the component of the magnetic field normal to the

grain boundary. The mobility of electrons in the layer at the boundary was quite high (of the order of 10^4 cm^2/Vs), enabling observation of the Shubnikov-de Haas oscillations in magnetic fields as low as $0.2T$. Two or three periods of the oscillations were observed, indicating again that several electric subbands were occupied by 2d electrons.

The electron concentrations and effective masses at the Fermi level were determined for each of the subbands and are listed in Table I. They are compatible with results of a calculation based on the model to be described in the following section. The results of this calculation are also listed in Table I. No spin splittings of the Landau levels were observed in the Shubnikov-de Haas oscillations studied in the samples of $Hg_{1-x}Mn_xTe$ ($x \approx 0.1$). This fact is due to the smallness of electronic g-factor, which at low temperatures, is greatly reduced by the exchange interaction in this open-gap material. This arises because the large and negative contribution to the g-factor due to the spin-orbit interaction is nearly compensated by the exchange induced terms proportional to the magnetization. Parenthetically, this fact enabled a precise determination of the effective masses from the temperature study of the oscillation amplitude.

To avoid the compensation of the g-factor, Grabecki *et al.* (1985) prepared also samples from quaternary $Hg_{1-x-y}Cd_xMn_yTe$ ($x = 0.23$, $y = 0.02$) containing the grain boundaries. The energy gap in these samples (≈ 200 meV) is open mainly by the presence of the Cd atoms. The effects of the exchange interaction due to the presence of the small number of Mn atoms are here more pronounced than in $Hg_{1-x}Mn_xTe$ ($x \approx 0.1$), because the reduction of the magnetization in the latter material is greater. This results from a stronger antiferromagnetic coupling between localized Mn moments in the less diluted case. In fact, the Shubnikov-de Haas oscillations of the 2d electrons in $Hg_{1-x-y}Cd_xMn_yTe$ samples show well-resolved spin splittings in the available range of magnetic fields. This enabled the first determination of the g-factor of the 2d electrons in a diluted magnetic semiconductor. Not surprisingly, the g-factor observed showed a strong temperature dependence (see Fig. 9). It is also well accounted for by the model of the subband structure (see next section). The effective mass at the Fermi level and the population of the lowest electric subband (only one period of oscillation was observed) in $Hg_{1-x-y}Cd_xMn_yTe$ are given in Table I.

7. Energy Levels of 2d Electron Gas

The model described below is based on semiclassical WKB approximation. It has been shown by Zawadzki (1983) that this simple approach can give a correct insight into the complex scheme of energy levels of a two-dimensional electron gas in narrow-gap semiconductors. Here we present a simplified

TABLE I

EXPERIMENTAL AND THEORETICAL VALUES OF 2d ELECTRON CONCENTRATION, n_s^r AND THE EFFECTIVE MASSES AT THE FERMI LEVEL (ε_F) m_r^* IN THE r-TH ELECTRIC SUBBAND IN SAMPLES CONTAINING GRAIN BOUNDARY. ε_r IS THE CALCULATED VALUE OF THE BOTTOM ($n_s^r = 0$) OF THE r-TH SUBBAND. THE FITTED VALUE OF THE POTENTIAL SLOPE U_0 IS GIVEN. THE SPATIAL EXTENSION OF THE r-TH STATE, W_r, WAS ESTIMATED FROM $W_r = \varepsilon_r/U_0$

	Experimental				Theoretical					
SAMPLE	E_g (meV)	r	n_s^r (10^{11} cm^{-2})	m_r^*/m_0 (10^{-2})	n_s^r (10^{11} cm^{-2})	m_r^*/m_0 (10^{-2})	ε_r (meV)	W_r (Å)	ε_F (meV)	U_0 (eV/cm)
$Hg_{0.89}Mn_{0.11}Te$	110	0	15.4 ± 2	5.0 ± 1	12.18	3.60	57.2	163		
		1	6.0 ± 0.5	3.3 ± 0.5	5.98	3.01	111.8	319	172	$7.0\ 10^4$
		2	1.8 ● 0.2	2.2 ± 0.2	1.87	2.40	151.3	432		
$Hg_{0.90}Mn_{0.10}Te$	85	0	5.3 ± 0.3	2.6 ± 0.2	5.29	2.49	52.7	192		
									122	$5.5\ 10^4$
		1	1.3 ± 0.1	2.0 ± 0.1	1.34	1.85	102.1	371		
$Hg_{1-x-y}Cd_xMn_yTe$ ($x = 0.23$, $y = 0.02$)	205	0	3.2 ± 0.1	2.6 ± 0.4	3.2	2.4	44.2	161	80.9	$5.5\ 10^4$

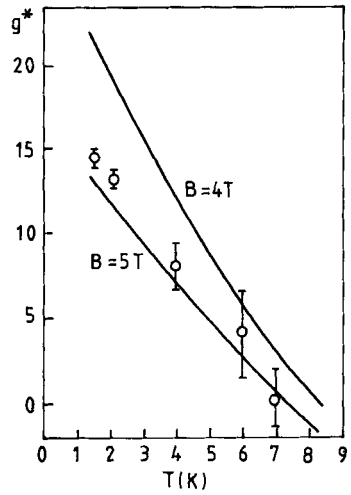

FIG. 9. The g-factor of 2d electrons at a grain boundary in $Hg_{0.75}Cd_{0.23}Mn_{0.02}Te$ as a function of the temperature. The symbols with error bars represent experimental data, based on the splitting of the magnetoresistance maximum at approximately $H = 4.5T$. Solid lines show the results of the calculation based on the model described in the text. [After Grabecki *et al.* (1985).]

version of the model, neglecting the presence of the spin-orbit split-off band Γ_7, aiming at the analytic form of solutions. Actual calculations, the results of which are given in Table I, were done without making this approximation. However, the influence of the higher bands was neglected in both versions. We start with the Hamiltonian in the matrix form given by Eqs. (13)–(16) with $\gamma_1 = \gamma_2 = \gamma_3 = F = \kappa = 0$.

The presence of the confining potential at the surface or at the grain boundary requires an addition of an appropriate potential U to the diagonal terms of these matrices. When the z-axis is chosen perpendicular to the surface (or to the grain boundary), the confining potential depends only on z. In the present model, very simple forms of this potential were assumed. In the case of the surface layer, the potential was taken to be a triangular well with infinite height on the insulator side; in the case of the grain boundary, it was assumed in the form of a symmetric triangular potential well. The slope of the potential is the only fitting parameter of the model. The other band structure parameters can be taken from electronic studies of bulk crystals. This simple form of the confining potential is probably the most severe approximation of the model. We assume also that the magnetic field is parallel to the z-axis. Finally, the exchange terms involving the constants α and β must be added to the Hamiltonian. The matrices obtained in this way represent two sets of differential equations for the envelope functions. These

functions can be sought in a factorized form $\Phi(x, y)\phi(z)$, with the dependence on x, y variables separated from the z variable. Moreover, $\Phi(x, y)$ can be chosen as a harmonic oscillator wave function, as in the case of Landau quantization. Thus we are left with a set of differential equations involving only d/dz, i.e., the z-component of the momentum p_z.

In the spirit of the semiclassical approximation, we may now treat p_z as a classical quantity. It can be then expressed in the following form (neglecting small terms proportional to $[U, p_z]$, $x\beta\langle S_z\rangle Pp_z/E_g^2\hbar$ and $x\beta\langle S_z\rangle E_g$):

$$[p_z^{\pm}(z)]^2 = \frac{a_0^{\pm}}{A}, \tag{33}$$

where

$$A = \frac{2}{3}\frac{P^2}{\hbar^2}, \tag{34}$$

$$a_0^{\pm} = [\varepsilon \pm \alpha' - \varepsilon_{\parallel}^{\pm} - U(z)]\left[E_g + \varepsilon_{+}^{-}\frac{\beta'}{3} + \varepsilon_{\parallel}^{\pm} - U(z)\right]. \tag{35}$$

In Eqs. (34) and (35), P denotes the interband momentum matrix element and

$$\alpha' = \tfrac{1}{2}x\alpha\langle S_z\rangle, \tag{36}$$

$$\beta' = \tfrac{1}{2}x\beta\langle S_z\rangle, \tag{37}$$

while ε denotes the eigenvalue of energy that we are looking for. Plus and minus indices in Eqs. (33) and (35) refer, respectively, to solutions for predominately spin-up and spin-down states in the conduction band. The parameter $\varepsilon_{\parallel}^{\pm}$ is defined by

$$\varepsilon_{\parallel}^{\pm} = -\frac{1}{2}\left[E_g \pm \left(\alpha' - \frac{\beta'}{3}\right)\right] + \frac{1}{2}\left\{\left[E_g \pm \left(\alpha' - \frac{\beta'}{3}\right)\right]^2 + 4X^{\pm}\right\}^{1/2}, \tag{38}$$

with

$$X^{\pm} = \frac{4}{3}\frac{P^2}{s}\left[n + \frac{1}{2} \mp \frac{1}{4} \pm \frac{\beta'}{3E_g}\left(n + \frac{1}{2} \mp 1\right)\right], \tag{39}$$

where $n = 0, 1, \ldots$ denotes the Landau quantum number, and $s = (\hbar c)/(eH)$.

The WKB quantization condition can be written in our case as

$$\int_{z_a}^{z_0} p_z\, dz = \hbar\pi(r + \phi), \qquad r = 0, 1, 2, \ldots \tag{40}$$

where $z_a = 0$ and $\phi = \frac{3}{4}$ for the case of the surface layer potential, while $z_a = -z_0$ and $\phi = \frac{1}{2}$ for the layer at the grain boundary. Here z_0 denotes the classical turn point of the motion in a confining potential well, i.e., it is

defined by

$$p_z(z_0) = 0 \tag{41}$$

The smallest root of Eq. (41) corresponds to solutions for the conduction band

$$z_0^{\pm} = \frac{\varepsilon \pm \alpha' - \varepsilon_{\parallel}^{\pm}}{U_0} \tag{42}$$

where we have explicitly used the form of the potential assumed

$$U(z) = \begin{cases} U_0 z, & z > 0 \\ \infty, & z \leq 0 \end{cases} \tag{43}$$

for the surface layer, and

$$U(z) = U_0|z| \tag{44}$$

for the grain boundary potential. The integration indicated by Eq. (40) can be carried out analytically, giving the following equations

$$4\sqrt{\frac{2}{3}}\frac{P}{G}U_0\pi(r+\phi) = (a^{\pm}+b^{\pm})\sqrt{a^{\pm}b^{\pm}} + (b^{\pm}-a^{\pm})^2 \ln\left|\frac{\sqrt{b^{\pm}}-\sqrt{a^{\pm}}}{\sqrt{b^{\pm}a^{\pm}}}\right|, \tag{45}$$

where

$$a^{\pm} = \varepsilon \mp \alpha' - \varepsilon_{\parallel}^{\pm}, \tag{46}$$

$$b^{\pm} = E_g + \varepsilon + \varepsilon_{\parallel}^{\pm} \mp \frac{\beta'}{3}, \tag{47}$$

and

$$G = \begin{cases} 1 & \text{for the surface layer} \\ 2 & \text{for the grain boundary layer} \end{cases}. \tag{48}$$

Equation (45) has now to be solved numerically for the energies of the n-th Landau level with spin (+) or (−) in the r-th electric subband.

A similar calculation can be carried out when no external magnetic field is applied. The result is formally very similar to that obtained for InSb, with the quantity $\varepsilon_{\parallel}^{\pm}$ redefined (cf., Zawadzki 1983):

$$\varepsilon_{\parallel}^{\pm} = -\frac{E_g}{2} + \left[\frac{E_g^2}{4} + E_g\frac{\hbar^2 k_{\parallel}^2}{2m_0^*}\right]^{1/2}, \tag{49}$$

where $m_0^* = \hbar^2(4P^2/3E_g)^{-1}$ and $k_{\parallel}$ is the momentum within the 2d layer. Solving Eq. (45) with the definition (49) of $\varepsilon_{\parallel}^{\pm}$, we may calculate the position

of the Fermi level ε_F^r related to the electron concentration n_s^r in the r-th subband.

$$n_s^r = \frac{1}{2\pi} k_\parallel^2. \tag{50}$$

By calculating the derivative of ε_F^r with respect to $k_\parallel$, we may calculate the effective mass at the Fermi level. Theoretical values of the effective mass listed in Table I were calculated in this manner. By choosing a proper value of the potential slope U_0, one can now fit the electron concentrations in each of the observed subbands and the effective masses to the experimental data, assuming a single Fermi level. A fair agreement can be reached indicating a proper choice of the shape of the potential (and its slope) at the grain boundary. By solving Eq. (45) with $\varepsilon_\parallel^\pm$ given by Eq. (38) for a fixed magnetic field, one can finally determine the value of the g-factor of the nth Landau level as

$$g^* = \frac{1}{\mu_B H} (\varepsilon_{rn}^+ - \varepsilon_{rn}^-). \tag{51}$$

The g-factors calculated in this way give a fairly good description of the values observed in $Hg_{1-x-y}Cd_xMn_yTe$. At lower temperatures, they turn out to be positive due to the large contribution of the exchange interaction terms. As T increases (and $\langle S_z \rangle$ decreases), the value of the g-factor drops, becoming nearly zero at the highest temperatures at which the oscillations were studied. Let us mention also that the values of the g-factor for the 2d gas of electrons at the grain boundary are slightly different from those expected for bulk electrons. The above results indicate that the influence of the localized magnetic moments also manifest itself in the properties of 2d electrons in diluted magnetic semiconductors.

8. Future Possibilities

Other 2d electronic systems in diluted magnetic semiconductors, e.g., those in quantum wells produced by heterostructures and/or superlattices, seem to offer quite interesting possibilities. One of those, noted by von Ortenberg (1982), makes use of the temperature and magnetic field variation of the band edges. Thus, if a superlattice is grown with alternating layers of nonmagnetic (e.g., $Hg_{1-x}Cd_xSe$) and diluted magnetic (e.g., $Hg_{1-x}Mn_xSe$) semiconductors, then it should in principle be possible to change the relative position of the band edges in adjacent layers by means of varying the field and/or the temperature. It is argued that the resulting minigap of a superlattice could be tuned by these external factors. However, such possibilities are still be be explored.

References

Abrahams, E. (1955). *Phys. Rev.* **98**, 387.

Adler, M. S., Hewes, C. R., and Senturia, S. D. (1973). *Phys. Rev.* **B7**, 5186.

Anderson, P. W. (1961). *Phys. Rev.* **124**, 41.

Ando, T., Fowler, A. B., and Stern, F. (1982). *Rev. Mod. Phys.* **54**, 437.

Bastard, G., Rigaux, C., Guldner, Y., Mycielski, J., and Mycielski, A. (1978). *J. de Physique* **39**, 87.

Bhattacharjee, A. K., Fishman, G., and Coqblin, B. (1983). *In* "Physics of Semiconductors" (Proc. 16th Internat. Conf. on the Physics of Semiconductors, Montpellier, 1982, M. Averous, ed.) **Part I**, p. 449, North Holland, Amsterdam.

Blom, F. (1980). *In* "Narrow Gap Semiconductors Physics and Applications" (W. Zawadzki, ed., Proceedings International School, Nimes, 1978, *Lecture Notes in Physics*, vol. **133**, p. 191, Springer-Verlag).

Blom, F. A. P., Neve, J. J., and Nouwens, P. A. M. (1983). *In* "Physics of Semiconductors" (M. Averous, ed., Proc. 16th Internat. Conf. Montpellier, 1982) **Part I**, p. 470, North Holland, *Physica* **117-118** B+C).

Bodnar, J. (1978). *In* "Physics of Narrow Gap Semiconductors" (J. Rauluszkiewicz, M. Gorska, E. Kaczmarek, eds., Proceedings of International Conference, Warsaw, 1977) p. 311, P.W.N. Publishers.

Byszewski, P., Szlenk, K., Kossut, J., and Galazka, R. R. (1979). *Phys. Stat. Sol. (b)* **95**, 359.

Byszewski, P., Cieplak, M. Z., and Mongird-Gorska, A. (1980). *J. Phys.* **C13**, 5383.

Delves, R. T. (1963). *J. Phys. Chem. Solids* **24**, 885.

Delves, R. T. (1966). *Proc. Phys. Soc.* **87**, 809.

Dobrowolska, M., Dobrowolski, W., Galazka, R. R., and Kossut, J. (1979). *Solid State Commun.* **30**, 25.

Dobrowolska, M., and Dobrowolski, W. (1981). *J. Phys.* **C14**, 5689.

Dobrowolska, M., Dobrowolski, W., Galazka, R. R., and Mycielski, A. (1981). *Phys. Stat. Sol. (b)* **105**, 477.

Elsinger, G. (1983). Thesis, Montanuniversität Leoben, unpublished.

Friedel, J. (1958). *Nuovo Cimento* **52**, 287.

Gaj, J. A., Planel, R., and Fishman, G. (1979). *Solid State Commun.* **29**, 435.

Galazka, R. R., and Kossut, J. (1980). *In* "Narrow Gap Semiconductors Physics and Applications" (W. Zawadzki, ed., Proc. Internat. School, Nimes, 1979) Lecture Notes in Physics, vol. **133**, p. 245, Springer-Verlag.

Galazka, R. R., and Kossut, J. (1983). *In* "Landolt-Börstein New Series," Group III (O. Madelung, M. Schulz, and H. Weiss, eds.) vol. **17b**, p. 302, Springer-Verlag.

Grabecki, G., Dietl, T., Kossut, J., and Zawadzki, W. (1984a). *Surf. Sci.* **142**, 588. (Proc. 5th Internat. Conf. on Electron Properties of Two-Dimensional Systems, Oxford, 1983.)

Grabecki, G., Dietl, T., Sobkowicz, P., Kossut, J., and Zawadzki, W. (1984b). *Appl. Phys. Lett.* **45**, 1214.

Grabecki, G., Dietl, T., Sobkowicz, P., Kossut, J., and Zawadzki, W. (1985). *Acta Phys. Polon.* **A67**, 297.

Hass, K. C., and Ehrenreich, H. (1983). *J. Vac. Sci. Technol.* **1**, 1678.

Irkhin, Yu. P. (1966). *Zh. Eksp. Teor. Fiz.* **50**, 379. (*Sov. Phys. JETP* **23**, 253.)

Izyumov, Yu. A., and Noskova, L. M. (1962). *Fiz. Tverdogo Tela* **4**, 217. (*Sov. Phys. Solid State* **4**, 153.)

Jaczynski, M., Kossut, J., and Galazka, R. R. (1978). *Phys. Stat. Sol. (b)* **88**, 73.

Kacman, P., and Zawadzki, W. (1971). *Phys. Stat. Sol. (b)* **47**, 629.

Kane, E. O. (1957). *J. Phys. Chem. Solids* **1**, 249.

Kaplan, T. A., and Lyons, D. H. (1963). *Phys. Rev.* **129**, 2072.
Karczewski, G., and Kowalczyk, L. (1983). *Solid State Commun.* **48**, 653.
Kasuya, T. (1955). *Progr. Theor. Phys.* **16**, 45, 58.
Kasuya, T. (1966). *In* "Magnetism" (G. T. Rado, and H. Suhl, eds.) vol. **2B**, p. 215.
Kasuya, T., and Lyons, D. H. (1966). *J. Phys. Soc. Japan* **21**, 287.
Kildal, H. (1974). *Phys Rev.* **B10**, 5082.
Kossut, J. (1976). *Phys. Stat. Sol. (b)* **78**, 537.
Kossut, J. (1978). *Solid State Commun.* **27**, 1237.
Leung, W., and Liu, L. (1973). *Phys. Rev.* **B8**, 3811.
Liu, S. H. (1961). *Phys. Rev.* **121**, 451.
Luttinger, J. M. (1956). *Phys. Rev.* **102**, 1030.
Luttinger, J. M., and Kohn, W. (1955). *Phys. Rev.* **97**, 869.
Lyapilin, I. I., Ponomarev, A. I., Kharus, G. I., Gavaleshko, N. P., and Maryanchuk, P. D. (1983). *Zh. Eksp. Teor. Fiz.* **85**, 1638. (*Sov. Phys. JETP* **58**, 953.)
Lyapilin, I. I., and Karyagin, V. V. (1980). *Fiz. Tverdogo Tela* **22**, 206. (*Sov. Phys. Solid State* **22**, 118.)
Mitchell, A. H. (1957). *Phys. Rev.* **105**, 1439.
Morrissy, C. (1973). Ph.D. Thesis, Oxford, unpublished.
Mycielski, A., Kossut, J., Dobrowolska, M., and Dobrowolski, W. (1982). *J. Phys.* **C15**, 3293.
Neve, J. J., Bouwens, C. J. R., and Blom, F. A. P. (1981). *Solid State Commun.* **38**, 27.
Neve, J. J., Kossut, J., van Es, C. M., and Blom, F. A. P. (1982). *J. Phys.* **C15**, 4895.
Niewodniczanska-Zawadzka, J., Kossut, J., Sandauer, A., and Dobrowolski, W. (1982). *In* "Physics of Narrow Gap Semiconductors" (E. Gornik, H. Heinrich, and L. Palmetshofer, eds., Proc. Internat. Conf. Linz, 1981) *Lecture Notes in Physics*, vol. **152**, p. 326, Springer-Verlag.
Niewodniczanska-Zawadzka, J., Elsinger, G., Palmetshofer, L., Lopez-Otero, A., Fantner, E. J., Bauer, G., and Zawadzki, W. (1983). *In* "Physics of Semiconductors" (M. Averous, ed., Proc. 16th Internat. Conf. Montpellier, 1982) part **I**, p. 458, North Holland (*Physica* **117–118** B + C).
von Ortenberg, M. (1982). *Phys. Rev. Lett.* **49**, 1041.
Pascher, H., Fantner, E. J., Bauer, G., Zawadzki, W., and von Ortenberg, M. (1983). *Solid State Commun.* **48**, 461.
Pastor, K., Grynberg, M., and Galazka, R. R. (1979). *Solid State Commun.* **29**, 739.
Pidgeon, C. R., and Brown, R. (1966). *Phys. Rev.* **146**, 575.
Ponikarov, B. B., Tsidilkovskii, I. M., and Shelushinina, N. G. (1981). *Fiz. Tekh. Poluprov.* **15**, 296. (*Sov. Phys. Semicond.* **15**, 170.)
Reifenberger, R., and Schwarzkopf, D. A. (1983). *Phys. Rev. Lett.* **50**, 907.
Roth, L., and Argyres, P. (1966). *In* "Semiconductors and Semimetals" (R. K. Beer, and A. C. Willardson, eds.) vol. **1**, p. 159, Academic Press.
Sandauer, A. M., and Byszewski, P. (1982). *Phys. Stat. Sol. (b)* **109**, 167.
Sandauer, A. M., Dobrowolski, W., Kossut, J., and Galazka, R. R. (1983). *In* "Physics of Semiconductors" (M. Averous, ed., Proc. 16th Internat. Conf. Monpellier, 1982) part **I**, p. 455, North Holland (*Physica* **117–118** B + C).
Sawicki, M., Dietl, T., Plesiewicz, W., Sekowski, P., Sniadower, L., Baj, M., and Dmowski, L. (1982). *In* "Application of High Magnetic Fields in Physics of Semiconductors" (G. Landwehr, ed., Proc. Internat. Conf., Grenoble, 1982). Springer-Verlag.
Schrieffer, J. R., and Wolff, P. A. (1966). *Phys. Rev.* **149**, 491.
Seager, C. H. (1982). *In* "Grain Boundaries in Semiconductors" (H. J. Leamy, G. E. Pike, C. H. Seager, eds.) North Holland.
Semenov, Yu. G., and Shanina, B. D. (1981). *Phys. Stat. Sol. (b)* **104**, 631.

Stankiewicz, J., Giriat, W., and Bien, M. V. (1975). *Phys. Stat. Sol. (b)* **68**, 485.
Story, T., Lewicki, A., and Szczerbakow, A. (1985). *Acta Phys. Polon.* **A67**, 317.
Takeyama, S., and Galazka, R. R. (1979). *Phys. Stat. Sol. (b)* **96**, 413.
Toth, G., and Leloup, Y. Y. (1970). *Phys. Rev.* **B1**, 4573.
Uchida, S., Landwehr, G., and Bangert, E. (1983). *Solid State Commun.* **45**, 9869.
Vonsovskii, S. V., and Svirskii, M. S. (1964). *Zh. Eksp. Teor. Fiz.* **47**, 1354. (*Sov. Phys. JETP* **20**, 914.)
Vonsovskii, S. V., and Turov, E. A. (1953). *Zh. Eksp. Teor. Fiz.* **24**, 419.
Vul, B. M., and Zavaritskaya, E. T. (1979). *Zh. Eksp. Teor. Fiz.* **76**, 1089. (*Sov. Phys. JETP* **49**, 551.)
Wallace, P. R. (1979). *Phys. Stat. Sol. (b)* **92**, 49.
Watson, R. E., and Freeman, A. J. (1966). *Phys. Rev.* **152**, 566.
Watson, R. E., and Freeman, A. J. (1969). *Phys. Rev.* **178**, 725.
Wittlin, A., Knap, W., Wilamowski, Z., and Grynberg, M. (1980a). *Solid State Commun.* **36**, 233.
Wittlin, A., Grynberg, M., Knap, W., Kossut, J., and Wilamowski, Z. (1980b). *J. Phys. Soc. Japan* **49** (suppl. A), 635. (Proc. 15th Internat. Conf. Phys. Semicond. Kyoto, 1980.)
Yosida, K. (1957). *Phys. Rev.* **106**, 893.
Zawadzki, W. (1983). *J. Phys.* **C16**, 229.
Zener, C. (1951a). *Phys. Rev.* **81**, 440.
Zener, C. (1951b). *Phys. Rev.* **82**, 403.
Zener, C. (1951c). *Phys. Rev.* **83**, 299.